The EMBO Journal Vol. 20 No. 11 pp. 2723–2741, 2001

Ezrin is a downstream effector of trafficking PKC–integrin complexes involved in the control of cell motility

Tony Ng[1,2,3], Maddy Parsons[1], William E.Hughes[4], James Monypenny[5], Daniel Zicha[5], Alexis Gautreau[6], Monique Arpin[6], Steve Gschmeissner[7], Peter J.Verveer[8], Philippe I.H.Bastiaens[8] and Peter J.Parker[4]

[1]Richard Dimbleby Department of Cancer Research, St Thomas' Hospital, Lambeth Palace Road, London SE1 7EH, [2]Cell Biophysics Laboratory, [4]Protein Phosphorylation Laboratory, [5]Light Microscopy Laboratory and [7]Electron Microscopy Unit, Imperial Cancer Research Fund, 44 Lincoln's Inn Fields, London WC2A 3PX, UK, [6]Laboratoire de Morphogenese et Signalisation Cellulaires, UMR 144 CNRS/Institut Curie, 75248 Paris Cedex 05, France and [8]Cell Biology and Cell Biophysics Programme, EMBL, Meyerhofstrasse 1, D-69117 Heidelberg, Germany

[3]Corresponding author
e-mail: T.Ng@icrf.icnet.uk

T.Ng and M.Parsons contributed equally to this work

Protein kinase C (PKC) α has been implicated in β1 integrin-mediated cell migration. Stable expression of PKCα is shown here to enhance wound closure. This PKC-driven migratory response directly correlates with increased C-terminal threonine phosphorylation of ezrin/moesin/radixin (ERM) at the wound edge. Both the wound migratory response and ERM phosphorylation are dependent upon the catalytic function of PKC and are susceptible to inhibition by phosphatidylinositol 3-kinase blockade. Upon phorbol 12,13-dibutyrate stimulation, green fluorescent protein–PKCα and β1 integrins co-sediment with ERM proteins in low-density sucrose gradient fractions that are enriched in transferrin receptors. Using fluorescence lifetime imaging microscopy, PKCα is shown to form a molecular complex with ezrin, and the PKC-co-precipitated endogenous ERM is hyperphosphorylated at the C-terminal threonine residue, i.e. activated. Electron microscopy showed an enrichment of both proteins in plasma membrane protrusions. Finally, overexpression of the C-terminal threonine phosphorylation site mutant of ezrin has a dominant inhibitory effect on PKCα-induced cell migration. We provide the first evidence that PKCα or a PKCα-associated serine/threonine kinase can phosphorylate the ERM C-terminal threonine residue within a kinase–ezrin molecular complex *in vivo*.

Keywords: ERM/FLIM/migration/PKC/wound

Introduction

Of the protein kinase C (PKC) family of protein kinases, several isoforms including PKCα (Platet *et al*., 1998), PKCδ (Kiley *et al*., 1999) and PKCθ (Tang *et al*., 1997) have been implicated in promoting a cell migratory phenotype. Recently, we and others have shown an enhancement of haptotactic cell motility/invasiveness following overexpression of PKCα (Ng *et al*., 1999a; Sun and Rotenberg, 1999). The precise mechanism(s) by which the catalytic activity of PKC influences cell motility has yet to be defined but is likely to involve components of the focal complexes, the small GTPases (Rho, Rac and Cdc42) and actin cytoskeleton-binding proteins (reviewed by Zigmond, 1996). In MCF-7 breast cancer epithelial cells, the signal machinery that drives efficient cell migration towards extracellular matrix β1 integrin substrates is dependent upon the PKCα-catalysed recycling of the activated [ligand-occupied, monoclonal antibody (mAb) 12G10-reactive] pool of β1 integrin receptors (Ng *et al*., 1999a). Overexpression of PKCα in MCF-10A human breast cells enhances cell motility, which is subject to control by the small GTPase Rac1 (Sun and Rotenberg, 1999). By using dominant inhibitor constructs, the activity states of RhoA, Rac1 and Rab5 have been shown to influence 12-*O*-tetradecanoylphorbol-13-acetate (TPA)-induced disassembly/reassembly of actin stress fibres and focal adhesions in MDCK cells (Imamura *et al*., 1998). In NIH 3T3 cells, growth factor-induced Rac1 activation is sensitive to PKC inhibition, also placing PKC upstream of Rac in this cell system (Buchanan *et al*., 2000).

ERM proteins (ezrin, radixin and moesin) are F-actin-binding proteins that affect actin cytoskeletal turnover and hence the maintenance of cell shape and lamellipodial extension (Crepaldi *et al*., 1997; Lamb *et al*., 1997; reviewed by Mangeat *et al*., 1999; Bretscher *et al*., 2000). Depending on individual cell types, ERM proteins have been reported to be localized to different structures including microvilli, ruffles, filopodia, uropods, retraction fibres and cell adhesion sites (reviewed by Tsukita and Yonemura, 1999).

The crystal structure of a dormant moesin N-terminal FERM (band four-point-one, ezrin, radixin, moesin homology domains)–C-terminal tail complex reveals the C-terminal segment to be bound as an extended peptide masking a large surface of the FERM domain (Pearson *et al*., 2000). The activation of ERM proteins is mediated by both C-terminal threonine phosphorylation (T567 in ezrin, T564 in radixin and T558 in moesin) (Matsui *et al*., 1999; Nakamura *et al*., 1999; Gautreau *et al*., 2000; Pearson *et al*., 2000) and exposure to polyphosphoinositides (reviewed by Mangeat *et al*., 1999). *In vitro*, the T558-phosphorylated form of moesin interacts with F-actin only in the presence of polyphosphoinositides such as phosphatidylinositol 4,5-bisphosphate [PI(4,5)P_2] (Nakamura *et al*., 1999).

Two protein kinases, namely PKCθ (Pietromonaco *et al*., 1998) and Rho-kinase/ROCK (Matsui *et al*., 1998; Tran Quang *et al*., 2000), were found to phosphorylate the

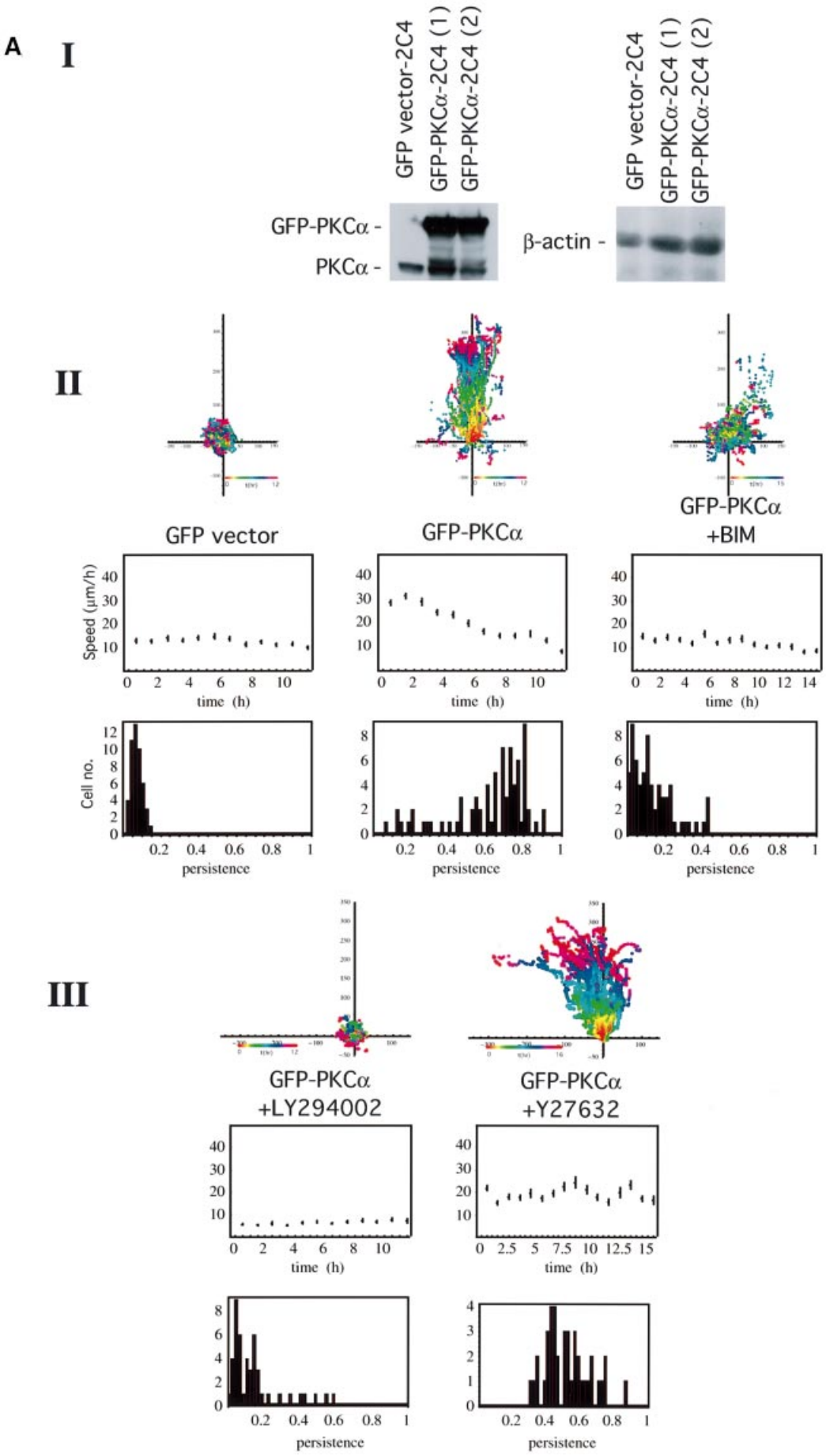
A
I
GFP vector-2C4
GFP-PKCα-2C4 (1)
GFP-PKCα-2C4 (2)
GFP-PKCα -
PKCα -
β-actin -
II
GFP vector
GFP-PKCα
GFP-PKCα +BIM
Speed (μm/h)
time (h)
Cell no.
persistence
III
GFP-PKCα +LY294002
GFP-PKCα +Y27632

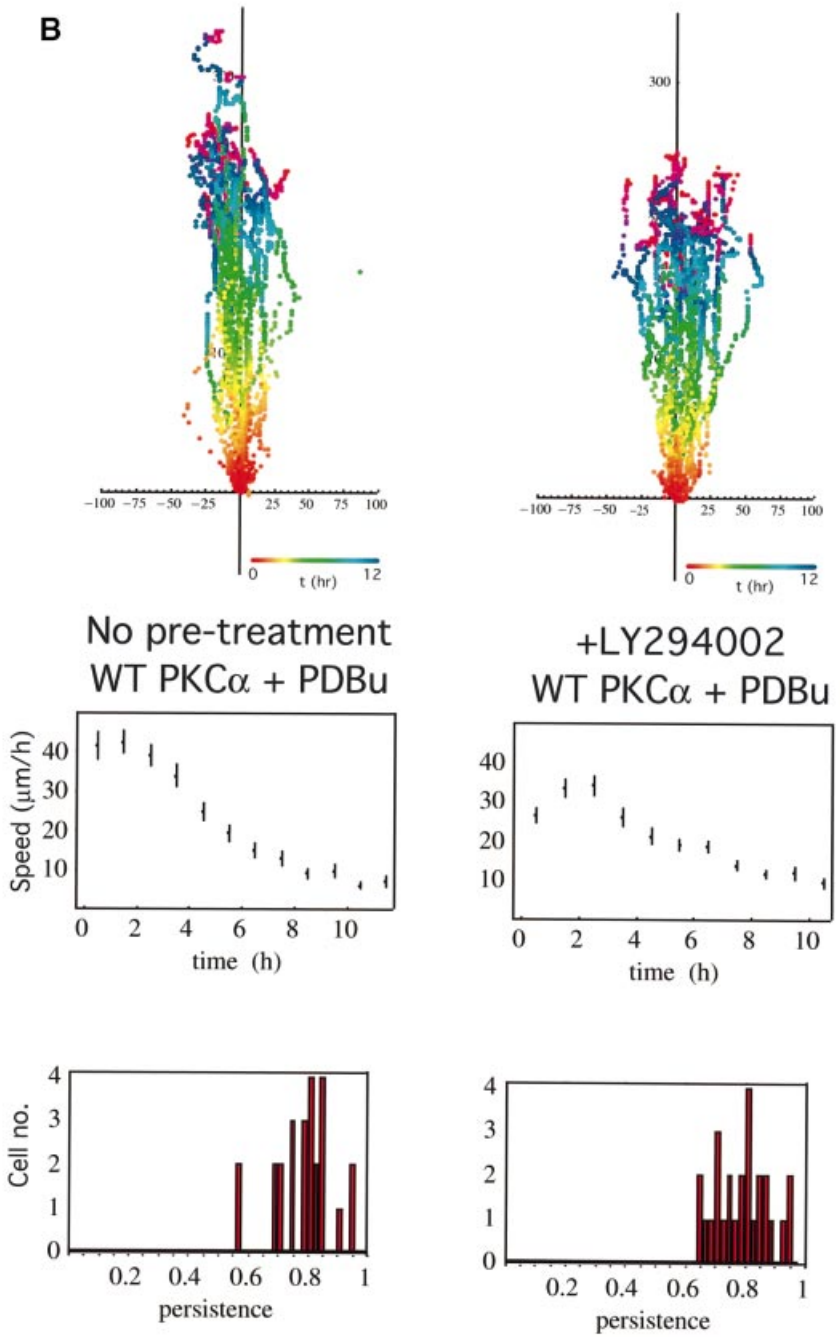

Fig. 1. PKC-driven wound closure response in 2C4 fibrosarcoma cells stably transfected with GFP–PKCα. (**A**) Confluent 2C4 fibrosarcoma cells stably transfected with GFP–PKCα (GFP–PKCα-2C4) or the GFP control vector were wounded and the wound closure response was recorded by time-lapse microscopy. Part I: the total level of PKCα, as detected by a PKCα C-terminal polyclonal antibody, in two different batches of the GFP–PKCα-2C4 cell line (1) and (2), in comparison with that in the vector control cell line. Loading control was provided by stripping the blot and reprobing with an anti-β-actin mAb. In both GFP–PKCα-2C4 lanes, both the exogenous GFP-tagged and untagged forms of PKCα are apparent, with the latter possibly representing a cleavage product of the expressed protein. Overall, the ratio of the levels of PKCα expressed in GFP–PKCα-2C4 versus the GFP control vector line was 3:1. In both parts II and III, the upper panels show all the cell trajectories during the entire time course of each experiment. Each dot represents a cell position at a particular time point that is indicated by the pseudocolour scale (*t* in h) beneath each set of cell tracks. The scale of the cell track axes is in μm. Middle panels show the changes in mean speed (of all tracked cells ± SD) with time, and the lower panels show the distribution of persistence within the cell populations in each treatment group. Speed and persistence were derived from the analysis of tracked cells from at least four independent experiments (except for the +Y-27632 data where $n = 2$) as described in Materials and methods. Persistence of motility measured for each cell was calculated as the ratio of the resultant displacement in 16 h over the sum of individual 5 min displacements. GFP–PKCα-2C4 cells (GFP–PKCα) ($n = 75$, mean persistence = 0.63 ± 0.2) showed a significant increase in persistence of migration into a wound space overnight ($P < 0.01$) when compared with 2C4 cells stably expressing GFP control vector (GFP vector) ($n = 48$, mean persistence = 0.08 ± 0.03). In cultures wounded in the presence of 10 μM BIM (GFP–PKCα + BIM) ($n = 66$, mean persistence = 0.14 ± 0.1) or LY294002 (10 μM) (GFP–PKCα + LY294002) ($n = 46$, mean persistence = 0.15 ± 0.14), there was a loss of cell persistence. The Rho kinase (ROCK) inhibitor Y-27632 (GFP–PKCα + Y27632) ($n = 40$, mean persistence = 0.53 ± 0.1) had no effect on the persistence of migration compared with untreated cultures. (**B**) GFP–PKCα-2C4 cells were wounded after a 30 min incubation in media containing LY294002 (10 μM) (+LY294002) ($n = 26$, mean persistence = 0.79 ± 0.09). PDBu (1 μM) was added to the media after wounding and the wound closure response was monitored. Results from two independent experiments were analysed. The *P*-value for the difference between the LY294002-treated group and the no pre-treatment control (WT PKCα + PDBu) ($n = 25$, mean persistence = 0.79 ± 0.09) was derived using ANOVA.

C-terminal threonine residue of the ERM proteins *in vitro*. However, the authors who first showed that ROCK phosphorylates the site *in vitro* (Matsui *et al*., 1998) subsequently reported that the C-terminal threonine phosphorylation of ERM is in fact insensitive to ROCK inhibition *in vivo* (Matsui *et al*., 1999). To date, the protein serine/threonine kinase(s) that is responsible *in vivo* for the phosphorylation of the ERM C-terminal threonine residue has yet to be identified.

In the present study, we have found both green fluorescent protein (GFP)–PKCα and β1 integrins to co-localize with endogenous ezrin *in vivo*. Using fluorescence lifetime imaging microscopy (FLIM) and co-immunoprecipitation, GFP–PKCα was confirmed to form a molecular complex with vesicular stomatitis virus (VSV) G-tagged ezrin in MCF-7 cells. The C-terminal threonine phosphorylation of ERM is dependent on the catalytic domain function of PKC (not ROCK) in an *in vivo* model of cell migration. Finally, a phosphorylation site mutant of ezrin that is incapable of interacting with the cytoskeleton but retains the ability to bind PKC is shown here to exert a dominant inhibitory effect on PKC-driven cell migration.

Results

PKC-enhanced cell migration in response to wounding

Previously we observed that transient expression of GFP–PKCα increased the haptotactic response of MCF-7 cells towards β1 (but not αvβ5) integrin substrates (Ng *et al*., 1999a). In this study, we confirmed that stable expression of a GFP–PKCα full-length construct also significantly enhanced the 'persistence' of 2C4 fibrosarcoma cell migration in response to wounding in comparison with cells stably expressing the corresponding GFP control vector [$P < 0.01$ by analysis of variance (ANOVA), Figure 1A].

The cumulative speed profile of GFP–PKCα-2C4 cells in Figure 1A showed faster cell movement than that of the vector control cell line during the initial 4 h post-wounding but, when the whole time course was analysed statistically, the speed of the GFP–PKCα-expressing cells based on 5 min displacements was not different from the speed of the control cells by ANOVA. The total level of PKCα expressed in GFP–PKCα-2C4 cells (which is a mixed clone), after correction with the β-actin control, was ~3 times that of the endogenous protein present in the vector control cells (Figure 1A). In GFP–PKCα-2C4 cell cultures wounded in the presence of the PKC inhibitor bisindolylmaleimide I (BIM, 10 μM) or the phosphatidylinositol 3-kinase (PI3K) inhibitor LY294002 (10 μM), there was a loss of the wound closure response ($P < 0.01$ by ANOVA for all three inhibitors, showing a significant loss of persistence of the wound closure response compared with no treatment control). Persistence of motility measured for each cell was calculated as the ratio of the resultant displacement in 16 h over the sum of individual 5 min displacements. The ROCK inhibitor Y-27632 had no effect on the wound-induced migratory response (persistence or speed) compared with untreated cultures ($P = 0.49$ by ANOVA showing no significant difference in persistence of the wound response compared with no treatment control). An analysis of the speed data by ANOVA, however, indicated a significant reduction in speed with LY294002 compared with no treatment control.

Activation of PKC with phorbol 12,13-dibutyrate (PDBu) treatment (post-wounding) was shown to reverse the inhibition of cell migration by LY294002 [$P = 0.096$ by ANOVA, comparing the wound migratory response following pre-treatment with LY294002 (+PDBu) with control treatment, i.e. +PDBu post-wounding alone; Figure 1B].

PKC control of ERM C-terminal phosphorylation in response to wounding

A monoclonal antibody (297S) that recognizes the C-terminal threonine-phosphorylated (T567 in ezrin, T564 in radixin and T558 in moesin; Nakamura *et al*., 1999) form of ERM proteins (CPERM) was used to monitor their phosphorylation in relation to PKC activation. In MCF-10A monolayer culture, endogenous PKCα redistributed to a vesicular compartment at the wound edge (Figure 2A). This redistribution was coincident with an increase in PKCα phosphorylation at the Thr250 site (Ng *et al*., 1999b), indicative of PKC activation at the wound edge (T.Ng, unpublished observations). Endogenous ERM protein phosphorylation at the C-terminal threonine residue is low in confluent monolayer cultures (observed for MCF-7, MCF-10A epithelial cells and GFP–PKCα-2C4 fibrosarcoma cell cultures) (Figures 2 and 3). An increase in ERM C-terminal threonine phosphorylation in response to wounding was observed at the wound edge. Pre-treatment of MCF-7 cells at the wound edge with alkaline phosphatase, following paraformaldehyde fixation, significantly reduced the recognition of endogenous ERM proteins by mAb 297S, confirming the phosphospecificity of the antibody (data not shown). The anti-CPERM staining partially co-localized with both the GFP-tagged and endogenous PKCα at the wound edge. The site of PKC/CPERM co-localization at the wound edge varied according to cell type. Co-localization was seen predominantly in intracellular vesicular structures in mammary epithelial cells such as MCF-10A and at cell ruffles in the case of 2C4 fibrosarcoma cells (Figure 2).

ERM C-terminal threonine phosphorylation at the wound edge was sensitive to PKC inhibition by BIM and PI3K inhibition by LY294002, but was not affected by the ROCK inhibitor Y-27632 (Ishizaki *et al*., 2000) (Figure 2). In 2C4 fibrosarcoma cells stably transfected with GFP–PKCα, the abrogation of the ERM C-terminal threonine phosphorylation by these inhibitors was mirrored by a reduction of the wound closure response (Figure 1A).

GFP–PKCα complexes with VSVG–ezrin in vivo

Of the ERM proteins, ezrin has been shown to be an effector of growth factor-mediated cell migration (Crepaldi *et al*., 1997). To determine whether ezrin forms part of the PKC–integrin complex, we assessed whether PKCα and ezrin associate upon PKC activation. FLIM was undertaken to determine the extent of fluorescence resonance energy transfer (FRET) between GFP–PKCα (donor) and VSVG-tagged ezrin stained with a Cy3 (acceptor)-conjugated antibody to the VSVG epitope. The spatial separation (R_0) between GFP and Cy3 at which the resonance energy transfer efficiency is 50% is 6 nm; however, detectable energy transfer can occur up to 9 nm

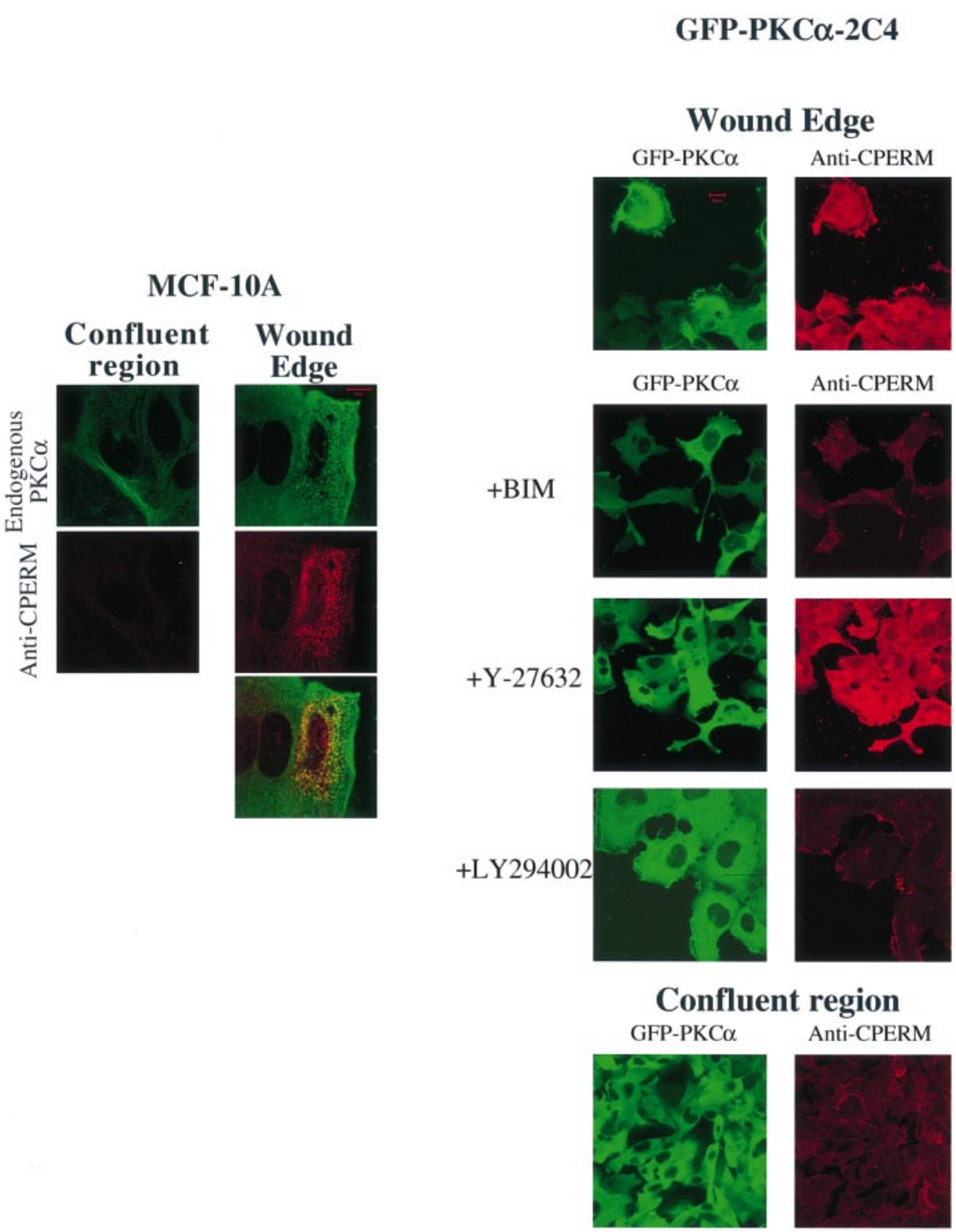

Fig. 2. PKC control of ERM C-terminal threonine phosphorylation in response to wounding. Confluent MCF-10A cells or 2C4 fibrosarcoma cells stably expressing GFP–PKCα (GFP–PKCα-2C4) were wounded and ERM C-terminal threonine phosphorylation (CPERM) was detected by confocal microscopy using an anti-CPERM mAb 297S as described in Materials and methods. Each image represents a two-dimensional projection of 2–3 slices in the Z-series, taken across the mid-depth of the cell at 0.2 μm intervals. Left: in wounded MCF-10A cells, endogenous PKCα was stained with mAb MC5 and its partial co-localization with anti-CPERM staining was shown. Representative scale bar = 10 μm. Right: GFP–PKCα-2C4 cells were pre-treated for 1 h and incubated with the following compounds for 4 h after wounding, before fixation: BIM (10 μM), LY294002 (10 μM) and ROCK inhibitor Y-27632 (10 μM). Representative scale bar = 20 μm. In both cell types, there was an increase in ERM C-terminal threonine phosphorylation (anti-CPERM) at the wound edge compared with the confluent region of the monolayer. The effects of the various inhibitors are shown.

(Ng *et al*., 1999b). FRET results in a shortening of the GFP (donor) fluorescence lifetime that is measured by two independent parameters, the phase shift (τ_p) and relative modulation depth (τ_m). Therefore, FRET should only be detected between two proteins that are closely associated or complexed *in vivo*.

When GFP–PKCα- and VSVG–ezrin-expressing cells were stained with VSVG-Cy3 following PDBu stimulation and fixation, it was evident that fluorescence lifetime, <τ>, measured as the average phase shift and relative modulation depth [$(\tau_p + \tau_m)/2$] for GFP was decreased at the plasma membrane and cell cortex beneath the membrane (Figure 3A). The presence of FRET (from GFP to Cy3) in these structures was confirmed by photobleaching the Cy3 acceptor, resulting in a lengthening of the donor <τ> after acceptor photobleaching (Figure 3C and data not shown). The FRET efficiency (Eff) pseudocolour plots, which only apply to the +anti-VSVG-Cy3 lifetime maps, give a qualitative indication of the pixel-to-pixel variation in the amount of PKC molecules that are complexed to ezrin. [Eff = $1 - \tau_{da}/\tau_d$ where τ_{da} is the lifetime map of the donor in the presence of acceptor and τ_d is the average lifetime of the donor in the absence of acceptor (average of the mean<τ> of at least five GFP–PKC alone control cells).] The efficiencies are approximately proportional to the fraction of the total steady-state fluorescence that originates from donor molecules in their bound state. Since the donor-tagged molecules transfer energy to the acceptor when they are in a complex, their lifetimes are reduced and hence the number of photons emitted would be reduced fractionally.

Statistical analysis of cumulative results from all the cells at each time point confirmed that there was a time-dependent, PDBu-enhanced association between GFP–PKCα and VSVG–ezrin [see two-dimensional lifetime histograms and pixel counts versus Eff (%) profile in the lower panels of Figure 3A]. The maximal levels of acceptor fluorescence intensity (anti-VSVG ezrin-Cy3) were similar in both untreated and PDBu-stimulated cells, and there was no significant correlation between <τ> and the intensity of acceptor fluorescence at each pixel of the cell (data not shown). The increase in association by PKC activation observed in Figure 3A is therefore not an artefact due to protein overexpression. Phorbol esters bind to the C1 domains of conventional and novel PKCs, and thereafter induce a conformational change that results in a disruption of the intramolecular interaction between the pseudosubstrate site in the regulatory domain (RD) and the kinase domain. Figure 3B shows that the expression of the PKCα RD + V3 (hinge region) alone, without the catalytic domain, renders the PKC–ezrin association constitutive. This implies that the PDBu effect is mediated at least in part through a conformational change in the PKC regulatory domain, and that the association is not merely a kinase domain–substrate binding.

The ezrin-bound and uncomplexed subpopulations of GFP–PKCα are associated with distinct fluorescence lifetimes (τ_1 and τ_2, respectively). Quantitative maps of the populations of each form were derived using a global FLIM analysis as previously described (Verveer *et al.*, 2000a,b), and two pseudocolour cell plots are presented in Figure 3B as 'percentage population of PKC complexed to ezrin'. A cumulative analysis of all the cell data showed that the average populations of the ezrin-complexed form of PKCα RD + V3 were 0.48 ± 0.08 (mean ± SD, $n = 7$; $\tau_1 = 0.56$ ns and $\tau_2 = 2.12$ ns) and 0.51 ± 0.12 ($n = 7$; $\tau_1 = 0.46$ ns and $\tau_2 = 2.06$ ns), before and after 20 min of PDBu treatment, respectively. This is in perfect agreement with the equivalent cumulative pixel counts versus Eff (%) profiles in the lowest panel, which show that PKC–ezrin association was rendered constitutive by expressing the RD + V3 alone. There is no linear relationship between the two quantities (i.e. populations versus Eff); hence, the contrast in the Eff cell plots in Figure 3B appears to be slightly different from the population images. Importantly though, the biological conclusions drawn from the cumulative/statistical analysis of these two parameters are identical.

Figure 3C shows that the non-phosphorylatable T567A mutant of VSVG–ezrin, which associates poorly with the actin cytoskeleton (Gautreau *et al.*, 2000; Tran Quang *et al.*, 2000), still interacts with PKCα. Cell morphology and the degree of PKC/ezrin co-localization were similar between wild-type and T567A ezrin-co-transfected cells, in agreement with previous observations made in LLC-PK1 cells (Gautreau *et al.*, 2000). Thus, phosphorylation at the C-terminal threonine residue is not a prerequisite for complex formation.

Co-sedimentation of GFP–PKCα and ezrin

Previously we found by cryoelectron microscopy that the 12G10-reactive β1 integrin localized to the filopodia and multivesicular bodies in breast carcinoma cells (Ng *et al.*, 1999a). In pulse–chase experiments coupled with immunofluorescence staining, the vesicular structures containing activated β1 integrins were shown to recycle and co-localize with transferrin receptors. By sucrose gradient fractionation, GFP–PKCα and β1 integrin were found to co-sediment through both velocity (VG) and equilibrium (EG) sucrose gradients prior to and following PDBu stimulation (Figure 5A and B and data not shown). Consistent with the FLIM results, in unstimulated MCF-7 cells there was no significant co-sedimentation between GFP–PKCα and endogenous ezrin (Figure 4A). In PDBu-stimulated cells, however, ezrin became highly enriched in PKCα- and β1 integrin-containing EG fractions (Figure 4B). Among the post-PDBu EG fractions, endogenous transferrin receptors were only detected in fractions 1–4, which were enriched in GFP–PKCα, β1 integrin and endogenous ezrin (data not shown), indicating that these fractions contained recycling endosomes.

T567 hyperphosphorylation of the PKCα-associated ezrin subpopulation

To corroborate the FLIM and sucrose gradient co-sedimentation data, we determined whether a PKCα–ezrin complex could be demonstrated by co-immunoprecipitation. Immunoprecipitation of endogenous PKCα from PDBu-stimulated MDA-MB-231 (which, unlike MCF-7, contains a sufficient amount of endogenous PKCα detectable by immunoblotting) with the antibody MC5 and western analysis with an anti-ezrin rabbit serum reveals that endogenous ezrin can be co-immunoprecipitated with PKCα (Figure 5A). The pool of ezrin in the PKCα-bound fraction was composed predominantly of a slower electrophoretic mobility form (labelled ezrin*) when compared with the unbound ezrin. The type of large resolving acrylamide gels used in these precipitation assays was shown previously to distinguish the mature phosphorylated form of PKCα (80 kDa) from its dephosphorylated variant (with an apparent mol. wt of 76 kDa) (Cazaubon *et al.*, 1994). Figure 5B shows a similar co-precipitation of

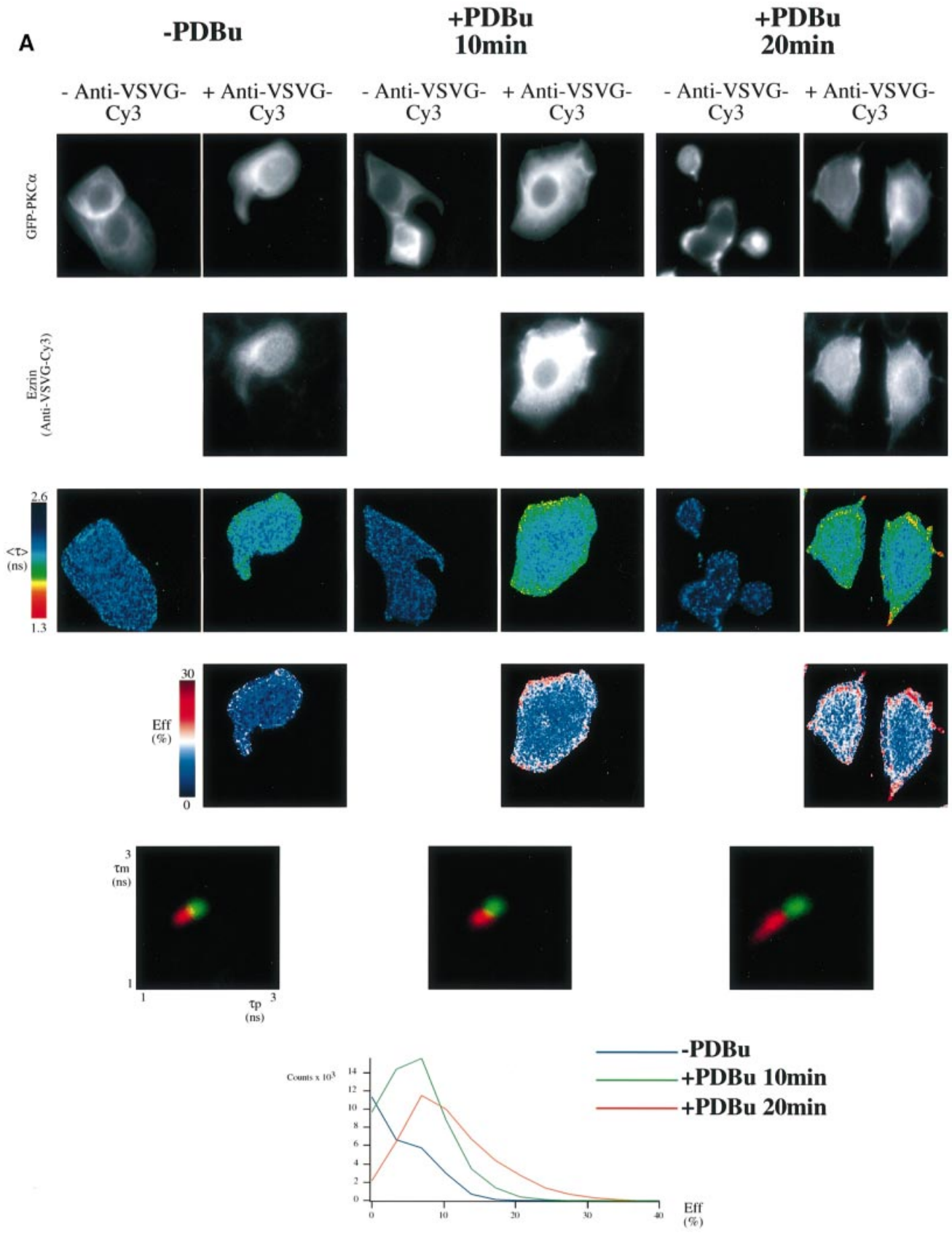

Fig. 3. (Continued over page)

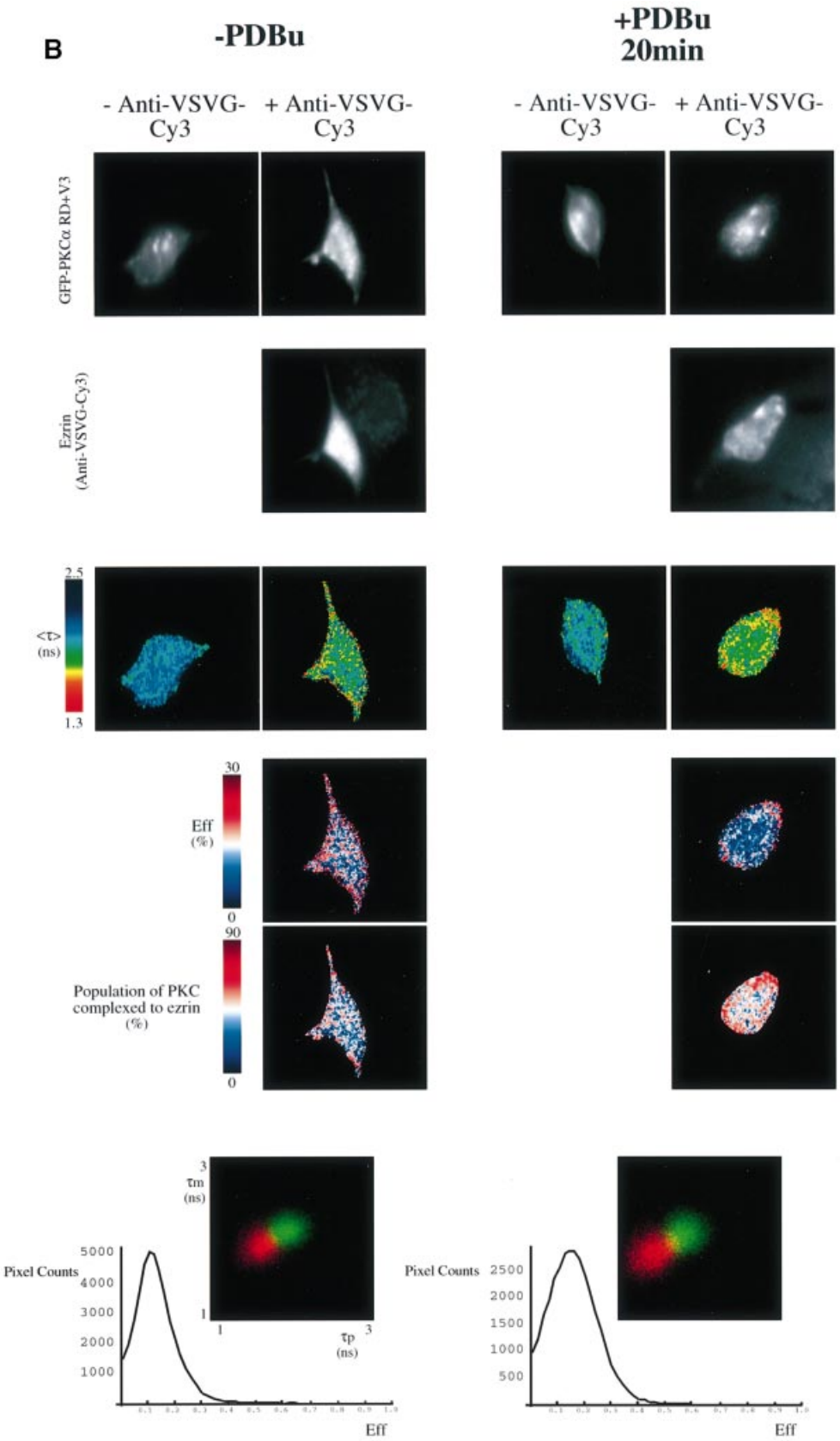

Fig. 3. PKC–ezrin association in MCF-7 cells detected by FLIM. (**A**) MCF-7 cells were dually transfected with both a GFP–PKCα- and a VSVG-tagged ezrin construct. After 36 h, cells were stimulated with PDBu (1 μM) for the times indicated, then fixed in ice-cold methanol for 4 min (–20°C). Cells were stained with a Cy3-labelled anti-VSVG mAb. FRET results in a shortening of the GFP (donor) fluorescence lifetime that is measured by two independent parameters, the phase shift (τ_p) and relative modulation depth (τ_m). The fluorescence images from the donor (GFP–PKCα) and acceptor (anti-VSVG-Cy3), the donor fluorescence lifetime <τ> (the average of τ_p and τ_m) and its corresponding pseudocolour scales are shown.

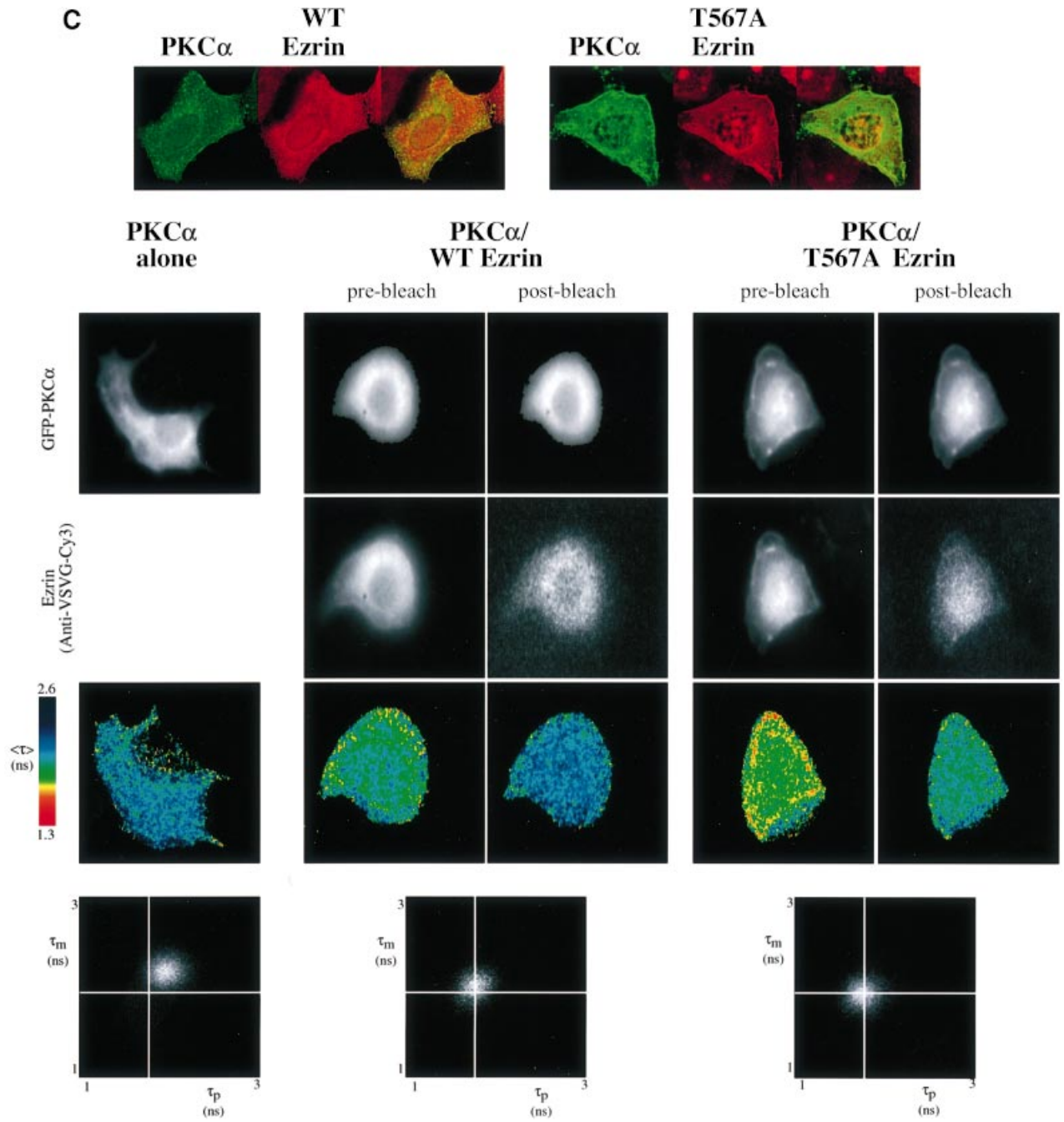

Eff is the pixel-by-pixel FRET efficiency represented on a pseudocolour scale [Eff = 1 – τ_{da}/τ_d, where τ_{da} is the lifetime map of the donor in the presence of acceptor and τ_d is the average lifetime <τ> of the donor in the absence of acceptor (numerically taken as the average of mean <τ> of five GFP–PKC alone control cells at each time point)]. The cumulative lifetimes of GFP–PKCα alone (green) and that measured in the presence of the acceptor fluorophore (red) are plotted on the two-dimensional histograms in the lower panels (n = 5 for each time point). The pixel counts versus Eff (%) profile in the bottom panel summarizes all the FRET efficiency data at each time point. (**B**) Repeat experiment in which MCF-7 cells were co-transfected with GFP–PKCα RD + V3 and wild-type VSVG–ezrin and stimulated with PDBu for 20 min before fixation. n = 7 for PDBu treatment and no treatment control. For cumulative analysis, in addition to the pixel counts versus Eff (%) profiles in the lowest panel, quantitative maps of the populations of both the ezrin-bound and unbound forms of GFP–PKCα RD + V3 were derived using a global FLIM analysis, and two representative pseudocolour cell plots are presented as 'percentage population of PKC complexed to ezrin'. (**C**) Repeat experiment in which MCF-7 cells were co-transfected with GFP–PKCα and either wild-type (WT) or T567A ezrin and stimulated with PDBu for 20 min before fixation. The confocal images in the upper panels are two-dimensional projections of 2–3 slices in the Z-series, taken across the mid-depth of the cell at 0.2 μm intervals, illustrating the similarity in terms of cell morphology and the degree of PKC/ezrin co-localization between WT and T567A ezrin-co-transfected cells. n = 4 for transfection with GFP–PKCα alone as well as for each PKC/ezrin co-transfection. Co-transfection with either WT or T567A ezrin and subsequent staining with the Cy3-labelled anti-VSVG antibody resulted in lifetime shortening (compared with GFP–PKCα alone controls), which was partially reversed after 4 min bleaching of the Cy3 acceptor as shown by the <τ> pseudocolor maps of the cells. The fluorescence images from the donor (GFP–PKCα) and acceptor (anti-VSVG-Cy3), before and after partial bleaching, are shown. Pre-bleach, before Cy3 acceptor photobleaching; post-bleach, after 4 min of photobleaching. The two-dimensional histograms represent the cumulative lifetimes.

GFP–PKCα with endogenous ezrin from PDBu-stimulated GFP–PKCα-2C4 cells, in two independent experiments (cultures 1 and 2); again the slow mobility form ezrin* was detected predominantly in the PKCα-bound fraction. The ratio of ezrin*:ezrin in the 'bound' fraction on the total ezrin blot in Figure 5B was 0.7 and 1.4 for cultures 1 and 2, respectively. An increase in the amount of the C-terminal threonine-phosphorylated form of ERM proteins (detected by an affinity-purified polyclonal rabbit anti-CPERM IgG) was found in the PKCα-bound pool, when compared with the unbound fraction. From densitometric analysis, the mean ratio of CPERM in PKC-bound versus unbound fraction ± SEM = 2.3 ± 0.3 (n = 7 independent cultures) and, when corrected for the total amount of ezrin present in each lysate, the mean ratio of CPERM in bound versus unbound ± SEM = 10.7 ± 3.1. The PKCα-associated ERM pool is therefore hyperphosphorylated at the C-terminal threonine residue. The phosphospecificity of this affinity-purified polyclonal IgG is demonstrated in Figure 5D.

The relative proportion of total ezrin/radixin/moesin bound to GFP–PKCα in unstimulated GFP–PKCα-2C4 cells was investigated by co-precipitation and is presented in Figure 5C. A comparison with Figure 5B and other similar experiments (n = 7 independent cultures) shows that in unstimulated cells, there is no C-terminal hyperphosphorylation of ERM in the PKC-associated fraction. The ezrin* band is not apparent under these conditions. A negligible amount of radixin was bound to PKCα. The stoichiometry of pull-down for moesin (PKCα-bound: unbound ~0.2) was less than that for ezrin (PKCα-bound:unbound ~0.7). Ezrin is therefore the predominant ERM protein that is associated with PKCα under these conditions.

Enrichment of GFP–PKCα and ezrin at plasma membrane protrusions

The precise localization of GFP–PKCα and ezrin was examined by immunoelectron microscopy (EM). Our initial efforts to localize PKCα by GFP immunogold labelling were unsuccessful using transiently transfected MCF-7 cells; the amount of endogenous ERM proteins in these cells was also below the detection limit using an affinity-purified rabbit anti-ezrin IgG (S.Gschmeissner and T.Ng, unpublished observations). A fibrosarcoma cell line stably expressing GFP–PKCα (GFP–PKCα-2C4) and transiently transfected with a VSVG-tagged ezrin was therefore chosen for EM studies. Electron micrographs in Figure 6A and B show the distribution of both VSVG-tagged ezrin [detected by an affinity-purified rabbit anti-ezrin IgG + 10 nm protein A–gold (PAG)] and GFP–PKCα (detected by a rabbit anti-GFP antiserum + 5 nm PAG) in the cytoplasm and plasma membrane of PDBu-stimulated GFP–PKCα-2C4 cells. Both proteins were found to be particularly enriched at plasma membrane protrusions. In contrast, there was no detectable labelling of other membranous structures including the mitochondria, Golgi and the nucleus. Control experiments where the second antibody (anti-GFP or anti-ezrin IgG) was omitted revealed no cross-reactivity of the 5 nm PAG with the first antibody (anti-ezrin or anti-GFP IgG, respectively) (data not presented). Figure 6C and D shows the immunolocalization of wild-type and T567A, VSVG-tagged ezrin in

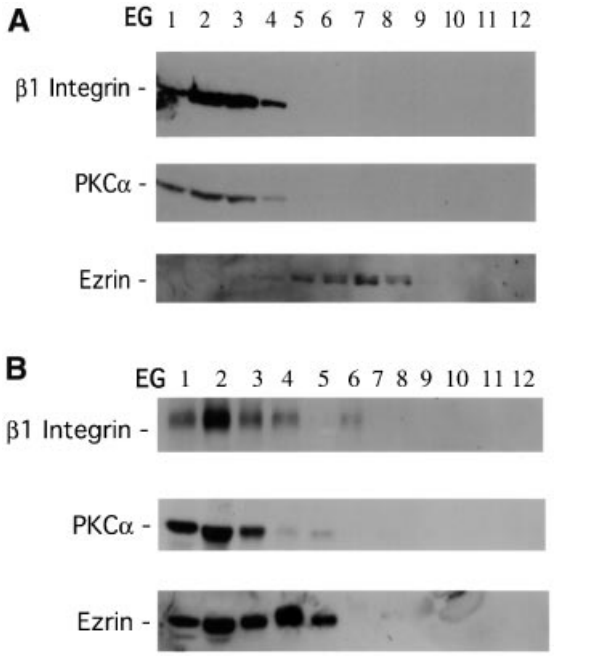

Fig. 4. Co-sedimentation of GFP–PKCα, β1 integrin and ezrin in sucrose gradient fractions derived from PDBu-activated MCF-7 cells. (**A**) PKCα and β1 integrin (recognized by mAbs MC5 and 8E3, respectively) were found in a light vesicle pool (fractions 2–3) from unstimulated, GFP–PKCα-transfected MCF-7 cell post-nuclear supernatant fractionated by velocity sucrose gradient (VG) centrifugation as described in Materials and methods (data not shown). Equilibrium gradient (EG) fractions were derived from this light vesicle pool (VG fractions 2–3) of unstimulated MCF-7 cell post-nuclear supernatant. EG fractions 1–4 were enriched in both GFP–PKCα and β1 integrin. There was a partial overlap with the EG fractions (4–8) containing endogenous ezrin. (**B**) The same as (A), with the exception that GFP–PKCα-transfected MCF-7 cells were stimulated with 1 μM PDBu for 10 min prior to fractionation. PKCα and β1 integrin were found to co-sediment in a light vesicle pool (fractions 2–3) from PDBu-stimulated, GFP–PKCα-transfected MCF-7 cell post-nuclear supernatant fractionated by VG centrifugation (data not shown). EG fractions were derived from these VGs. EG fractions 1–4 were enriched in GFP–PKCα and β1 integrin, as well as endogenous ezrin. Among the post-PDBu EG fractions, endogenous transferrin receptors were only detected in fractions 1–4 (data not shown).

GFP–PKCα-2C4 cells, respectively (stained with an anti-VSVG mAb P5D4 + 10 nm PAG). The distribution is remarkably similar. Also the distinction between the membrane- and cytoskeleton-associated subpopulations of wild-type versus T567 ezrin would be difficult, even at the EM level of resolution.

PKCα phosphorylates ezrin in vitro

The activation-enhanced association/proximity between PKCα and ezrin (Figure 3) as well as the significant diminution of ERM C-terminal threonine phosphorylation by PKC inhibition (Figure 2) suggest that ERM proteins may be *in vivo* substrates of PKCα. The only PKC isoform that has been documented to phosphorylate the ERM proteins *in vitro* to date is PKCθ (Pietromonaco *et al.*, 1998). Figure 7A shows that recombinant human PKCα can also phosphorylate full-length glutathione *S*-transferase (GST)-tagged ezrin *in vitro* in a Ca^{2+}/TPA/phospholipid-dependent manner. After 30 min of *in vitro* phosphorylation at 37°C, the stoichiometry was 1.5 mol ATP incorporated per mol ezrin. The ratio of ^{32}P

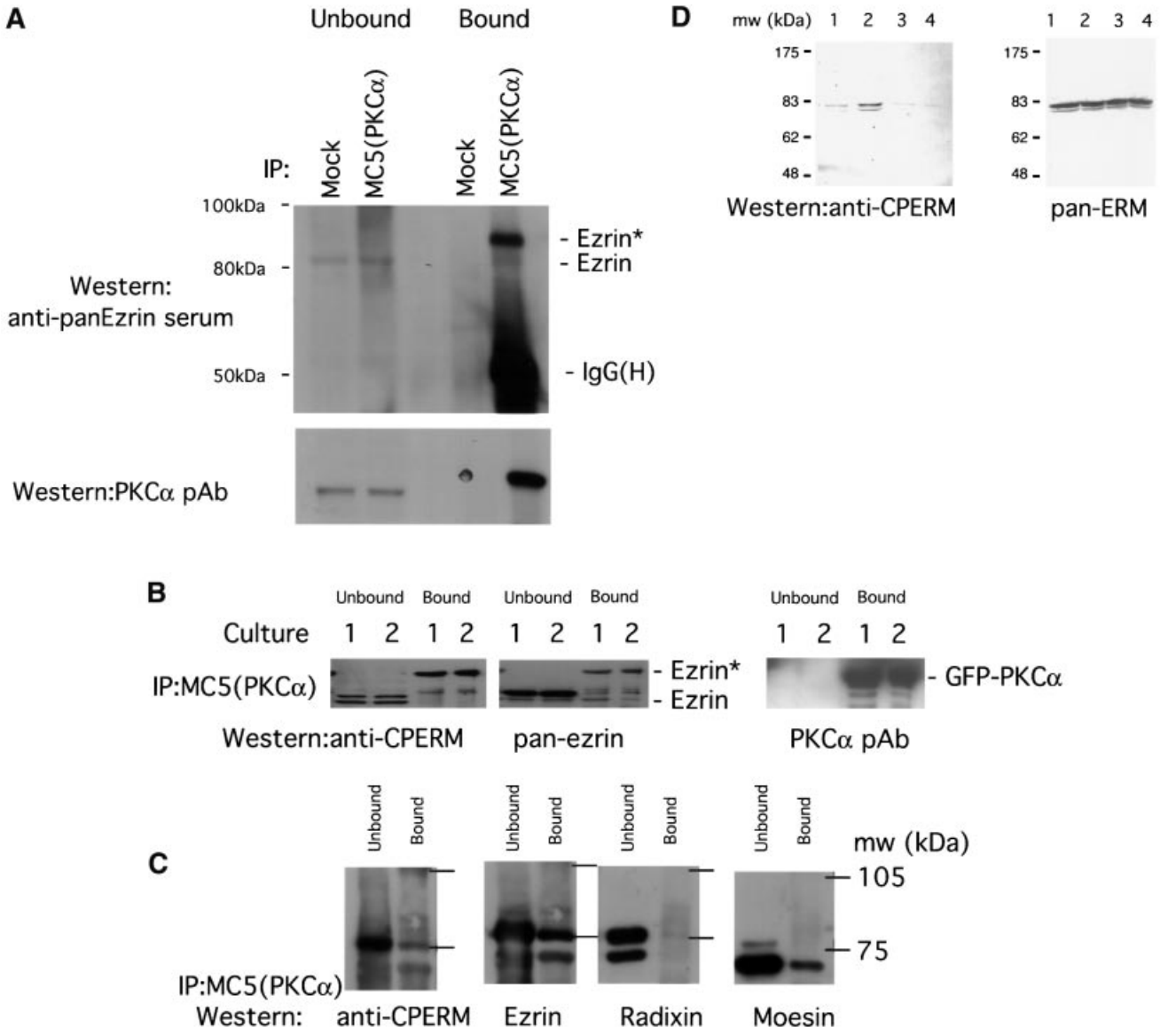

Fig. 5. Association of endogenous ERM proteins with PKCα *in vivo* correlated with an increase in C-terminal threonine phosphorylation. (**A**) MDA-MB-231 cells stimulated with PDBu. Co-precipitation of endogenous PKCα (immunoprecipitated with an anti-PKCα mAb MC5) with endogenous ezrin detected by an anti-ezrin rabbit serum. All the bound proteins on the protein G beads (bound) and 1/30 of the unbound proteins left in the cell extract supernatant after the first centrifugation post-precipitation (unbound) were loaded. Ezrin* is a subset of ezrin that exhibits a slower electrophoretic mobility and is only detected in the PKCα-bound ezrin pool. The blot was stripped and reprobed with an anti-PKCα pAb. Mock, control immunoprecipitation in which the precipitating antibody was omitted; IgG(H), immunoglobulin heavy chain. Approximate positions of the molecular weight markers are shown. (**B**) GFP–PKCα-2C4 cells stimulated with PDBu. Co-precipitation of GFP–PKCα with endogenous ezrin. All the bound proteins on the protein G beads (bound) and 1/100 of the unbound proteins left in the cell extract supernatant after the first centrifugation post-precipitation (unbound) were loaded. The blot containing MC5 immunoprecipitates, derived from two independent experiments (cultures 1 and 2), was detected first with a polyclonal rabbit anti-CPERM IgG, stripped and reprobed with an anti-ezrin rabbit serum, then stripped and reprobed again with an anti-PKCα pAb. (**C**) Relative proportion of total ERM bound to GFP–PKCα in unstimulated GFP–PKCα-2C4 cells. MC5 immunoprecipitates from three untreated cultures were pooled and one-third of the pooled bound proteins on the protein G beads (bound) were loaded. Similarly, 1/300 of the pooled unbound proteins left in the cell extract supernatant after the first centrifugation post-precipitation (unbound) were loaded. The blot was cut into three strips and stained with (i) an affinity-purified polyclonal rabbit anti-CPERM IgG and crude sera raised against radixin (ii) and moesin (iii), respectively. The anti-CPERM blot (i) was then stripped and reprobed with an affinity-purified anti-ezrin IgG that has been cross-adsorbed for moesin and radixin. (**D**) In total LLC-PK1 cell lysates, immunoreactivity of ERM proteins with the affinity-purified polyclonal rabbit anti-CPERM IgG was abolished by pre-treatment of cells with staurosporine (a broad spectrum protein kinase inhibitor) before cell lysis, and enhanced by calyculin A, a protein serine/threonine phosphatase 1 (PP1)/PP2A inhibitor. ERM, immunoblot developed with a mixture of antibodies specific for ERM (Gautreau *et al*., 2000). Lane 1, untreated; lane 2, treated with calyculin A (100 nM, 10 min); lanes 3 and 4, treated with 1 and 5 μM staurosporine, respectively, for 10 min. Approximate positions of the molecular weight markers are shown.

incorporation in ezrin ± PKC activators was ~3:1. Full-length ezrin was a better PKC substrate than the GST–C-terminal ezrin (amino acids 280–585) (<0.3 mol ATP incorporated per mol ezrin; data not shown), implying that components in the N-terminal part of ezrin might be required for kinase–substrate contact.

We next investigated the ability of immunoprecipitated PKCα to phosphorylate its associated endogenous ezrin at

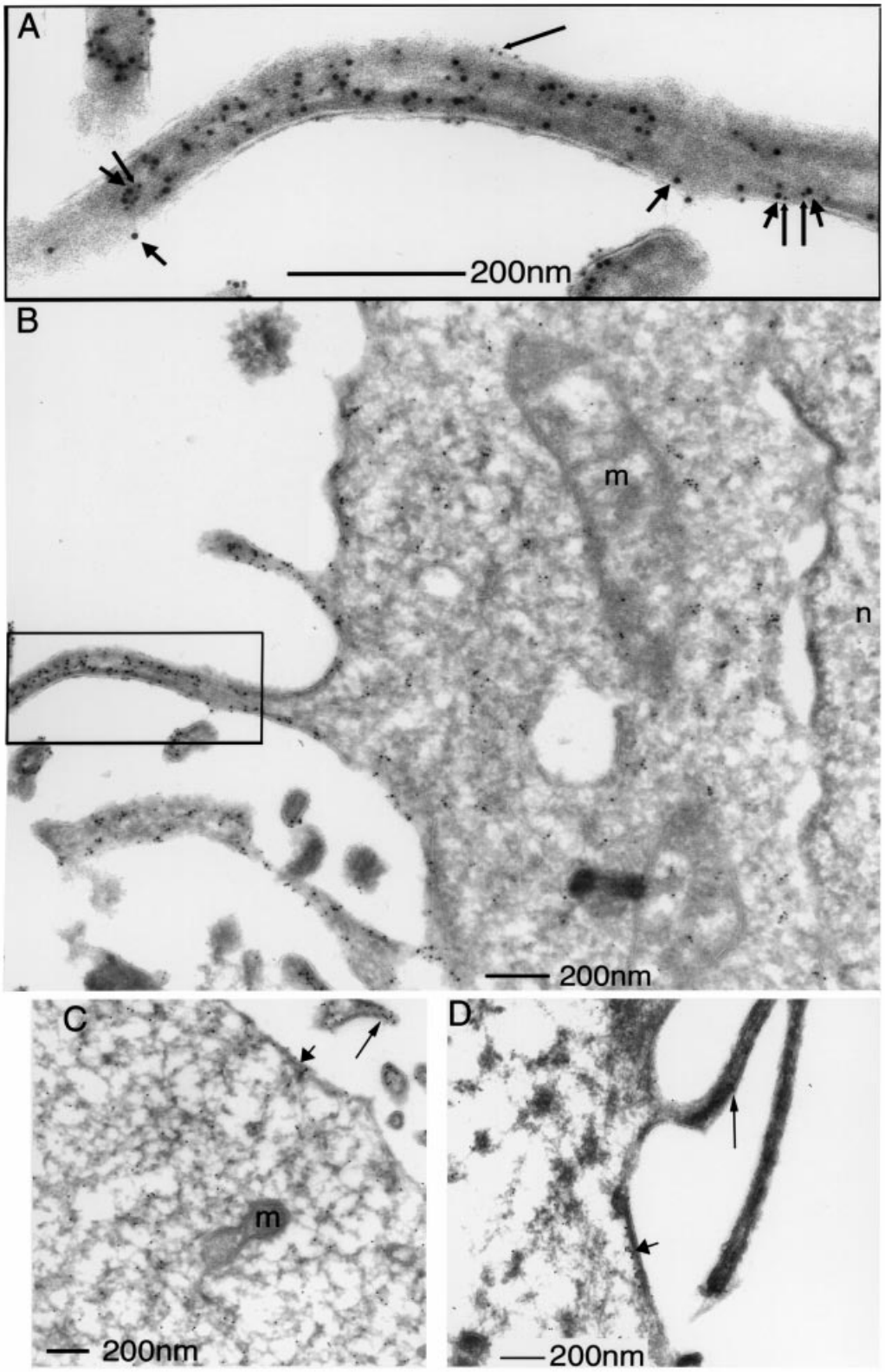

Fig. 6. Enrichment of GFP–PKCα and ezrin at plasma membrane protrusions. (A and B) The main immunoelectron micrograph (**B**) shows the localization of both VSVG-tagged ezrin (detected by an affinity-purified rabbit anti-ezrin IgG + 10 nm protein A–gold; short arrows) and GFP–PKCα (detected by a rabbit anti-GFP antiserum + 5 nm protein A–gold; long arrows). The inset (**A**) represents an enlarged view of a plasma membrane protrusion showing isolated and clusters of the 5 and 10 nm protein A–gold labels. m = mitochondrium, n = nucleus. (**C** and **D**) The immunolocalization of wild-type and T567A, VSVG-tagged ezrin in GFP–PKCα-2C4 cells, respectively (stained with an anti-VSVG mAb P5D4 + 10 nm protein A–gold). The long and short arrows show the localization of ezrin in the plasma membrane protrusion and a peripheral (cortical) area of the cell, respectively.

the C-terminal threonine residue *ex vivo* (procedure described in the legend of Figure 7B). In view of the findings in Figure 2, pre-treatment with LY294002 (10 μM for 6 h) was used to reduce the basal ERM C-terminal threonine phosphorylation in GFP–PKCα-2C4 cells, or more specifically in the PKCα-bound ERM proteins (–Mg/ATP, anti-CPERM 'bound' lane in Figure 7B). Notably, the PKC-associated ezrin* band was barely detectable in the total ezrin blot from cells pre-treated with LY294002 when compared with the untreated cultures shown in Figure 5B. After the *ex vivo* phosphorylation reaction (+Mg/ATP, anti-CPERM 'bound' lane in Figure 7B), there was an ~3-fold increase in the amount of CPERM on beads, indicating that PKCα, or a PKCα-associated serine/threonine kinase, is capable of phosphorylating the ERM C-terminal threonine residue within a kinase–ezrin molecular complex.

In order to address further the identity of the CPERM that is bound to PKCα, the PKCα immunoprecipitation experiment was repeated with GFP–PKCα-2C4 cells that had been pre-treated with LY294002 (10 μM for 6 h) to reduce the basal ERM C-terminal threonine phosphorylation before lysis. Under conditions where ERM C-terminal threonine phosphorylation is reduced, the CPERM in the PKC-bound fraction had the same apparent molecular weight as that in the unbound fraction. Using a large resolving acrylamide gel, the major band in the anti-CPERM blot (indicated by a filled arrowhead in Figure 7C) co-migrated with the major band in the anti-ezrin blot (developed with an affinity-purified anti-ezrin IgG that has been cross-adsorbed for moesin and radixin; Algrain *et al*., 1993). Very little radixin that corresponds to the major radixin band in the unbound fraction was found in the PKCα immunoprecipitate. The major moesin band had a similar apparent molecualr weight but the stoichiometry (PKCα-bound:unbound ~0.1) of pull-down was less than that for ezrin (PKCα-bound:unbound ~0.2). Ezrin is therefore also the predominant ERM protein that remains associated with PKCα under conditions where ERM C-terminal threonine phosphorylation is reduced.

Ezrin T567A mutant inhibits PKCα-driven migration in wound closure

To investigate the role of ERM proteins in PKCα-dependent migration, GFP–PKCα-2C4 cells transiently co-expressing ezrin (wild-type/T567A variant) were tracked during overnight wound migration assays. The T567A mutant of VSVG–ezrin associates poorly with the actin cytoskeleton (Gautreau *et al*., 2000; Tran Quang *et al*., 2000) but retains the capacity to interact with PKCα *in vivo* (Figure 3C). Figure 8 demonstrates that the injection of a wild-type ezrin plasmid into GFP–PKCα-2C4 cells did not affect the PKCα-stimulated wound closure response. However, introduction of the T567A phosphorylation site mutant had a dominant inhibitory effect on PKCα-induced cell migration (P = 0.02 by ANOVA for the difference between wild-type- and T567A ezrin-injected cells, showing a significant loss of persistence of the wound closure response due to T567A ezrin expression). There was no significant cell toxicity associated with T567A ezrin expression, as assessed by the propidium iodide exclusion assay (data not shown).

Discussion

The results here demonstrate that on activation, PKCα co-localizes and interacts with ezrin at the plasma membrane and cell cortex beneath the membrane, particularly at the membranous protrusions of the cell. Associated with this interaction, ERM proteins become phosphorylated on the C-terminal threonine residue, and agents that block this phosphorylation also abrogate PKCα-dependent migration. In addition, PKC-associated endogenous ERM proteins are shown to be hyperphosphorylated preferentially at the C-terminal threonine residue, i.e. activated. Among the endogenous ERM proteins, ezrin is the predominant ERM protein that is associated with PKCα. Recombinant human PKCα is capable of phosphorylating full-length GST-tagged ezrin *in vitro* in a Ca^{2+}/TPA/phospholipid-dependent manner. Full-length ezrin is a better PKC substrate than the GST–C-terminal ezrin, implying that components in the N-terminal part of ezrin might be required for stabilizing kinase–substrate contact. The expression of the regulatory domain of PKCα alone is sufficient to support this interaction. We have also provided the first evidence that PKCα, or a PKCα-associated serine/threonine kinase, is capable of phosphorylating the ERM C-terminal threonine residue within a kinase–ezrin molecular complex in cells.

The pool of ERM proteins bound to PKCα contains a higher proportion of the C-terminal threonine-phosphorylated form than the 'unbound' pool. The increase in C-terminal threonine phosphorylation in the bound fraction correlates with the finding of a subset of ezrin that is associated with a slower electrophoretic mobility (ezrin*). The increase in the apparent molecular weight of ezrin* is likely to be related to its phosphorylation by PKC (or a PKCα-associated serine/threonine kinase) within an intermolecular complex, as well as any additional biochemical modification that occurs as a consequence of the phosphorylation. This is because in unstimulated cells where there is no C-terminal hyperphosphorylation of ERM in the PKC-associated fraction (Figure 5C), or under conditions where ERM C-terminal threonine phosphorylation is reduced (Figure 7C), the CPERM in the PKC-bound fraction has the same apparent molecular weight as that in the unbound fraction. The ezrin* band is also not apparent under these conditions.

Recent work (Gautreau *et al*., 2000) clearly demonstrates that the C-terminal threonine-phosphorylated form is enriched in the membrane and exists as a monomer. One possible consequence of the C-terminal threonine phosphorylation within the PKC–ezrin molecular complex is therefore to promote a transition of ERM from the oligomeric to monomeric state (active form). The activated form of ERM then acts as a downstream effector of PKCα involved in the control of polarized cell movement. The observed dominant inhibitory effect of expressing the T567A mutant of ezrin on PKC-enhanced wound closure can be explained in a number of ways. First, the T567A variant has an almost identical cytosol/membrane distribution as the wild-type protein but associates poorly with the cytoskeleton (Gautreau *et al*., 2000). This is not surprising since the T567A variant can oligomerize with endogenous ERM proteins and localize to the same compartments in cells. The localization of the T567A

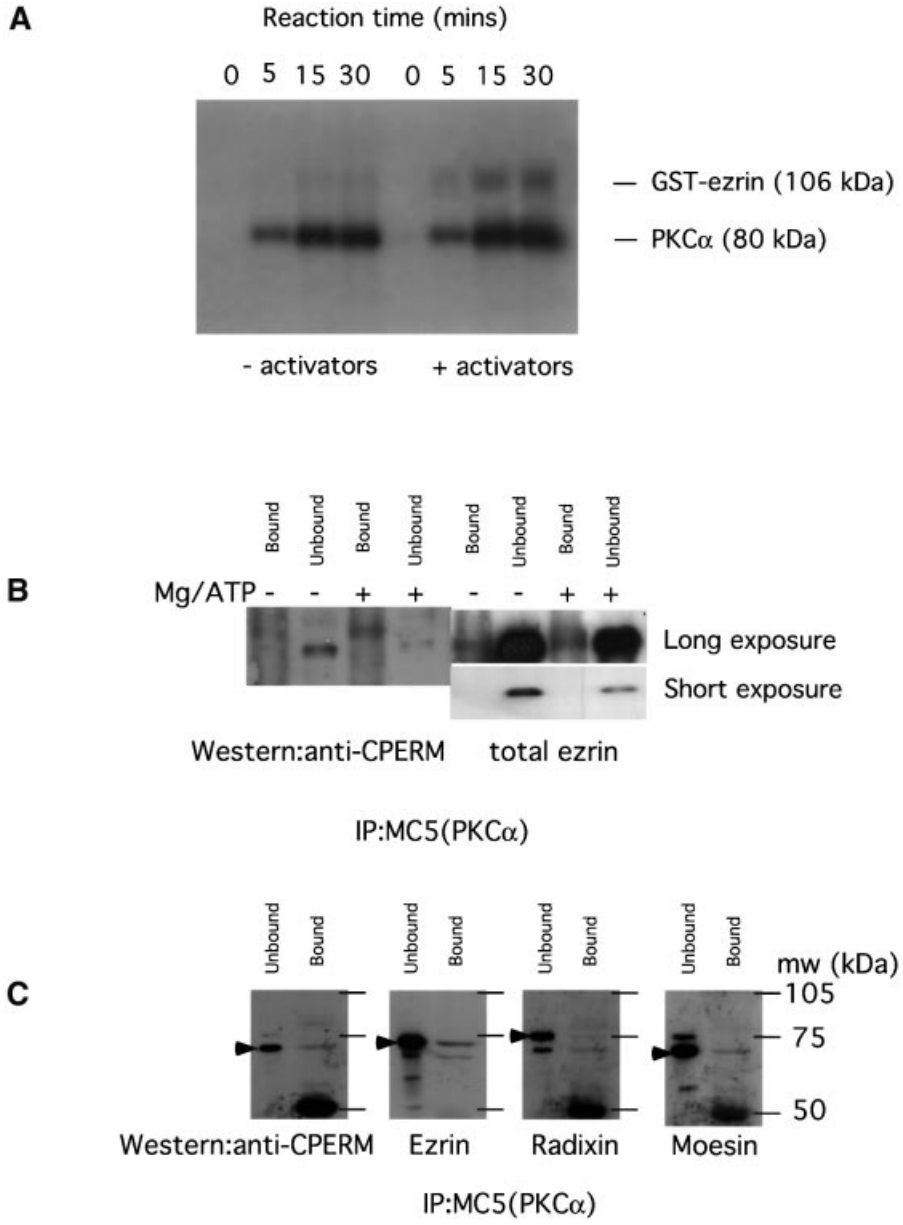

Fig. 7. *In vitro* phosphorylation of ezrin by PKCα. (**A**) *In vitro* phosphorylation of a GST–wild-type ezrin (106 kDa) with human recombinant PKCα was carried out as described in Materials and methods. The time courses of the autophosphorylation of PKCα and TPA/lipids/Ca^{2+} (activators)-induced, PKC-mediated ezrin phosphorylation (representative of >3 experiments) are shown. (**B**) GFP–PKCα was immunoprecipitated with an anti-PKCα mAb MC5 from whole-cell lysates of 80% confluent GFP–PKCα-2C4 cell monolayer cultures that were pre-treated for 6 h with LY294002 (10 μM). One-hundredth of the unbound proteins left in the cell extract supernatant after the first centrifugation post-precipitation were loaded in the lanes marked 'unbound'. The protein G beads were washed at 4°C, post-precipitation, twice with the modified RIPA buffer, then twice with 70 μl of a 0.05 M HEPES/0.5 mM EGTA buffer containing a cocktail of protease inhibitors, calyculin A (10 nM) and sodium orthovanadate (1 mM). In the +Mg/ATP lane, this was exchanged for an equivalent buffer containing in addition 12.5 mM $MgCl_2$ and 0.1 mM ATP. The beads were then incubated at 30°C for 30 min in a shaking heating block. The phosphorylation reaction was stopped by centrifugation in a cooling microcentrifuge (4°C) and by adding 70 μl of modified Laemmli's sample buffer (containing final concentrations of 2% SDS, 4 M urea and 10 mM EDTA) to the beads post-centrifugation. All the bound proteins on the protein G beads were loaded in the lanes marked 'bound'. Western blotting with the polyclonal rabbit anti-CPERM IgG showed an ~300% increase in the amount of CPERM in the PKC-co-precipitated material on beads after the *ex vivo* phosphorylation reaction. The amount of ezrin on beads (total ezrin) in the – Mg/ATP or +Mg/ATP lane was similar. The ratio of the 'bound:unbound total ezrin' was, however, notably lower in the LY294002-treated cultures (<0.2 in both the – Mg/ATP and +Mg/ATP lanes) compared with untreated cultures (mean ± SEM = 0.6 ± 0.08; Figure 5 and data not shown). A shorter exposure of the pan-ezrin blot shows that the amount of total ezrin in the 'unbound' fraction of the +Mg/ATP lane was slightly lower than that of the –Mg/ATP lane but these were derived from different cultures. (**C**) Repeat of the PKCα immunoprecipitation experiment with GFP–PKCα-2C4 cells that had been pre-treated with LY294002 (10 μM for 6 h) to reduce the basal ERM C-terminal threonine phosphorylation before lysis. One-hundredth of the unbound proteins left in the cell extract supernatant after the first centrifugation post-precipitation were loaded in the lanes marked 'unbound'. The protein G beads were washed at 4°C, post-precipitation, twice with the modified RIPA buffer, then once with a 10 mM Tris pH 7.4 buffer containing a cocktail of protease and phosphatase inhibitors before elution with 70 μl of Laemmli's sample buffer. All the bound proteins on the protein G beads were loaded in the lanes marked 'bound'. The blot was probed with an anti-CPERM IgG, then stripped and reprobed with an affinity-purified anti-ezrin IgG that had been cross-adsorbed for moesin and radixin, followed by anti-radixin and anti-moesin detection, respectively, with the appropriate rabbit sera. The major band of reactivity in each blot is indicated by a filled arrowhead. The approximate positions of molecular weight markers are shown and, after sufficient exposure times, a 50 kDa band appeared and corresponds to the immunoglobulin heavy chain.

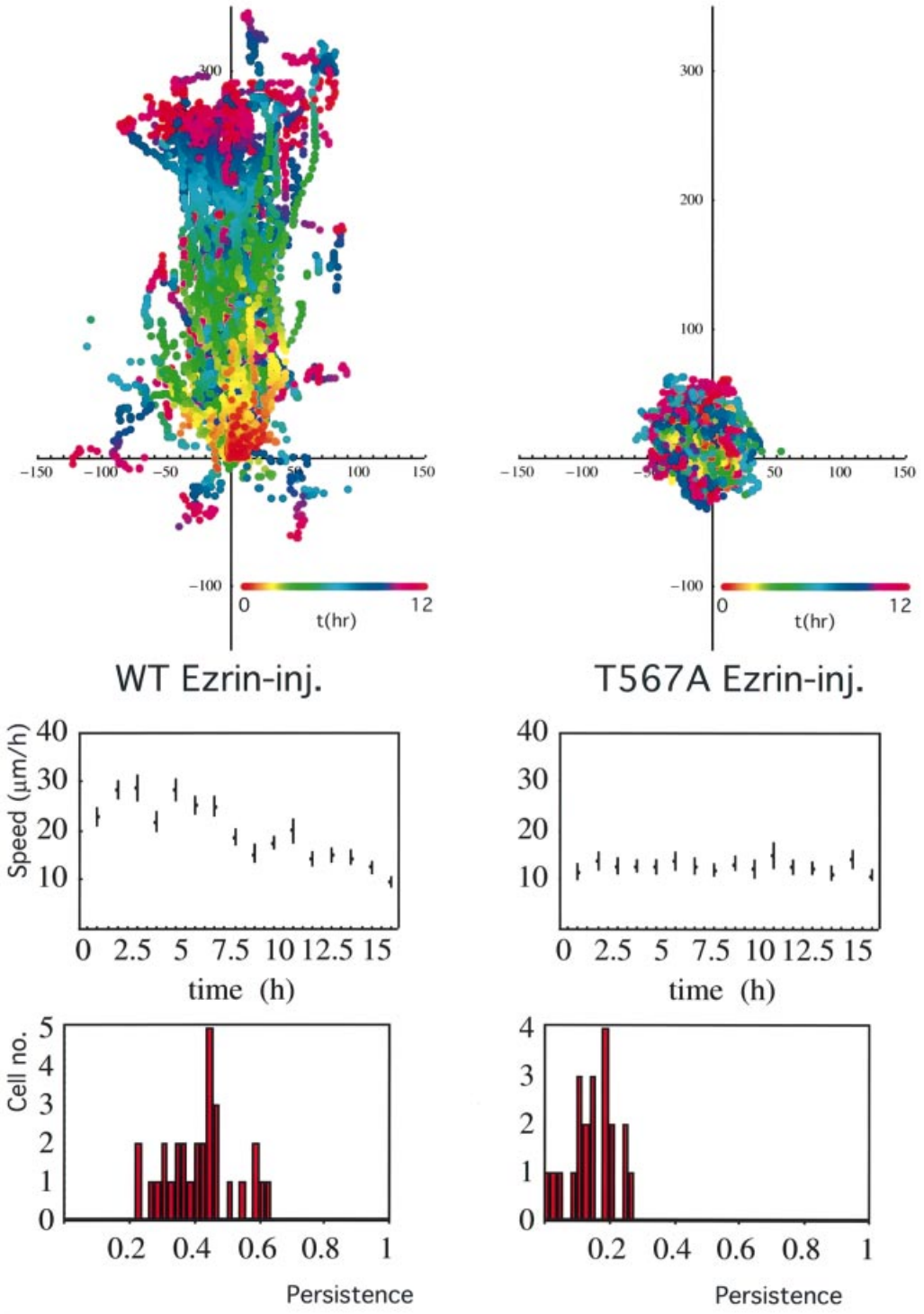

Fig. 8. Dominant inhibitory effect of the T567A ezrin variant on the PKCα-induced wound migratory response. A wild-type or T567A VSVG-tagged ezrin plasmid (100 μg/ml) was microinjected into the nuclei of confluent GFP–PKCα-2C4 cells along with a Cy3-conjugated anti-transferrin receptor antibody as a marker to identify the injected cells subsequently. The monolayer was wounded and the migration response was recorded by time-lapse microscopy. Upper panels: all the cell trajectories during the entire time course of each experiment. Each dot represents a cell position at a particular time point that is indicated by the pseudocolour scale (*t* in h) beneath each set of cell tracks. The scale of the cell track axes is in μm. Left, wild-type ezrin-injected cell (WT Ezrin-inj.); right, a representative T567A ezrin-injected cell (T567A Ezrin-inj.). Middle panel: the changes in mean speed with time. Lower panel: the distribution of persistence within the cell populations in each treatment group. Speed and persistence were derived from the analysis of tracked cells from three independent experiments (total number of cells tracked = 30 for WT Ezrin-inj. and 21 for T567A Ezrin-inj.). The mean persistences = 0.42 ± 0.1 (SD) and 0.15 ± 0.07 (SD) for the WT Ezrin-inj. and T567A Ezrin-inj. cultures, respectively. The *P*-value for the difference between the two treatment groups was derived using ANOVA.

variant is indistinguishable from that of the wild-type protein, even at the EM level (Figure 6). Through oligomerization with endogenous ERM proteins, this mutant may exert a dominant inhibitory effect by sequestering the active (C-terminally phosphorylated) form of ERM. Alternatively, since T567A ezrin will still interact with PKCα in intact cells, it may sequester the kinase away from foci of actin polymerization.

In MDCK cells, PKCα (not PKCδ or ζ) is the only PKC isotype that changes its cellular localization concomitantly with the development of Ca^{2+}-dependent desmosomes in response to wounding (Wallis *et al*., 2000). Treatment with an antisense oligonucleotide to PKCα abolishes the reversal of desmosomes to Ca^{2+} dependence at the wound edge, illustrating the important role that this specific PKC isozyme plays in the wounding response. The molecular mechanisms underlying the wound closure migratory response are, hitherto, poorly understood. After an overnight incubation, an intermediate zone of subconfluent cells is usually observed between the wound edge and the unperturbed part of the confluent monolayer culture. Cells in this subconfluent zone are motile and have less extensive intercellular contact than cells from the confluent region. PKC-induced wound closure (such as that shown in Figure 1A) is characterized by an increase in 'persistence' in the direction of cell movement, particularly in this intermediate zone where there is less contact inhibition of cell migration. Based on our previous work using the Transwell chamber migration sytem where the filter was coated with either bovine serum albumin (BSA; random motility) or specific integrin substrates (Ng *et al*., 1999a), the expression of PKCα in MCF-7 cells was observed significantly to enhance random motility as well as haptotaxis towards β1 integrin substrates on filters. Here we conclude that stable expression of a GFP–PKCα full-length construct significantly enhances the 'persistence' of 2C4 fibrosarcoma cell migration in response to wounding. GFP–PKCα-2C4 cells tend to undergo a more accelerated cell movement (speed) during the initial 4 h post-wounding in comparison with the vector control. Speed is a measure of random motility (Surtees, 1964) and is mathematically an entirely independent entity from persistence/directionality. These conclusions do not just apply to confluent cells induced to move in response to wounding, since the expression of PKCα in subconfluent MCF-7 cells also significantly enhances the directional cell movement in a chemotaxis assay (M.Parsons *et al*., in preparation).

ERM C-terminal phosphorylation at the wound edge is sensitive to PI3K inhibition with LY294002, but not the ROCK inhibitor Y-27632. The PKC-driven wound closure response is significantly impaired by these same inhibitors that abolish the ERM C-terminal threonine phosphorylation; this response is also insensitive to Y-27632. PI3K has long been implicated in the control of cell migration/haptotaxis (Wang *et al*., 1996; Derman *et al*., 1997; Shaw *et al*., 1997; Meng and Lowell, 1998; Ng *et al*., 1999a; Vanhaesebroeck *et al*., 1999). At least in NIH 3T3 fibroblasts, the di-C_{16}-phosphatidylinositol-3,4,5-trisphosphate (PtdIns-P_3)-induced cell motility involves PKC and can be inhibited by calphostin C (Derman *et al*., 1997). Also, in lymphocytes, PI3K blockade has an inhibitory effect on moesin redistribution to the uropod during migration (Vicente-Manzanares *et al*., 1999). Here we demonstrate that in a GFP–PKCα stably transfected fibrosarcoma cell line (GFP–PKCα-2C4), ERM C-terminal threonine phosphorylation, which is sensitive to inhibition of the catalytic activity of PKC *in vivo*, is also subject to PI3K control. PI3K may, by enhancing phospholipase C-γ activity *in vivo* (Bae *et al*., 1998), increase the availability of diacylglycerol (DAG), which in turn activates PKC and ERM phosphorylation. This would be consistent with the inhibitory effect that calphostin has (via competition for the DAG-binding site on PKC; Bruns *et al*., 1991) on PtdIns-P_3-induced cell motility (Derman *et al*., 1997). Furthermore, we show that activation of PKC with PDBu treatment can reverse the inhibition of the wound migratory response by LY294002, placing allosteric activation of conventional or novel PKC isozymes downstream of PI3K (Figure 1B). These data further define the functional relationship between PI3K and PKC as downstream effectors of the integrin signalling axes (Berrier *et al*., 2000). Finally, the p85 regulatory subunit of PI3K has been shown to bind to the N-terminal part of ezrin; a point mutant of ezrin that does not interact with PI3K has an inhibitory effect on the activation of Akt, a downstream effector of the PI3K pathway (Gautreau *et al*., 1999). This complex array of feedback mechanisms between PKC, PI3K and ezrin may constitute an important mechanism for signal amplification and cell migratory function.

The PKC isozymes constitute a major family of protein kinases that influence cell motility through a variety of mechanisms that are involved in the regulation of cytoskeletal turnover (Arber *et al*., 1998) and possibly microtubule function (Steiner *et al*., 1990). Some of the downstream components may, like ezrin, form stable complexes with PKC in response to appropriate physiological stimuli, while others, such as cofilin, may be regulated indirectly through other signalling proteins (Arber *et al*., 1998). Further studies are needed to integrate our current knowledge of these individual signal components in a physiological context with the aim of intervening in these PKC-dependent processes in a pathological milieu such as tumour cell metastasis.

Materials and methods

Cell culture and plasmid constructs

Human breast carcinoma cells (MCF-7 cells) were cultured in Dulbecco's modified Eagle's medium (DMEM) containing 10% fetal calf serum at 37°C, in a 10% CO_2 atmosphere. In addition, the MCF-7 cultures were grown in media supplemented with insulin (10 μg/ml). MCF-10A cells were established originally from mammary tissue of a patient with fibrocystic breast disease and display characteristics of luminal epithelial cells. Transient transfection was performed using Fugene (Boehringer Mannheim). 2C4 fibrosarcoma cells (derivative of HT1080 cells) were transfected with either GFP–PKCα plasmid (Ng *et al*., 1999a,b) or the control vector. At 48 h after transfection was initiated, cells were replated in complete medium at a 1:5 ratio. Selection for neomycin resistance was started the following day by the addition of the antibiotic G418 (Sigma) to 400 μg/ml. GFP-expressing cells were enriched by fluorescence activated cell sorting. After 10–14 days, G418-resistant cells were isolated as a mixed clone (see Figure 1A for the level of exogenous PKCα) and subsequently maintained in complete growth medium containing 40 μg/ml G418. Stable transfectants were cultured for up to 20 passages. The GFP–PKCα RD + V3 (Ng *et al*., 1999a) was made by subcloning the corresponding PKCα sequence encoding amino acids 1–337 into the pEGFP-N1 vector (Clontech), permitting fusion of the coding sequence of eGFP. The VSVG-tagged ezrin (wild-type and T567A variant) constructs were published previously (Gautreau *et al*., 2000).

Antibodies and direct conjugation to fluorophores, and Fab fragment generation

Anti-VSVG mAb was purchased from Boehringer Mannheim. MC5 is a murine mAb that recognizes the V3 region of PKCα (Young *et al*., 1988). 8E3 is a pan-β1 integrin murine mAb (a kind gift of M.Humphries). The rat mAb (297S) that recognizes the C-terminal threonine-phosphorylated (T567 in ezrin, T564 in radixin and T558 in moesin; Nakamura *et al*., 1999) form of ERM was a kind gift of S.Tsukita (Kyoto, Japan). A similar polyclonal rabbit anti-CPERM antibody was obtained by immunizing with a keyhole limpet haemocyanin (KLH)-coupled CRDKYKT*LRQIR peptide (the asterisk indicates the phosphorylated residue) and purifying the serum obtained through a GST–ezrin C(280–585) column to eliminate the non-phosphospecific antibodies. Phosphospecific antibodies were then affinity purified on a column coupled to the immunizing peptide. Goat polyclonal IgG against the C-terminus of ezrin was purchased from Santa Cruz and used in immunocytochemical staining. For western blotting, both a crude rabbit serum against ezrin and its affinity-purified IgG that has been cross-adsorbed for moesin and radixin (Algrain *et al*., 1993) were used. Also, crude sera raised against radixin and moesin (kind gifts of Professor Paul Mangeat, Universite Montpellier II) were used for blotting. Fab fragments were generated and isolated from mouse IgG using the ImmunoPure Fab preparation kit (Pierce) according to the manufacturer's protocol. Direct conjugation of IgG/IgG Fab fragments to the fluorophores Cy3 and Cy5 (Amersham Life Science) was performed at pH 8.5 (IgG) or pH 9.0 (IgG Fab) as described previously (Bastiaens and Jovin, 1998).

Wound migration assays

Cells were plated at confluence onto 22 mm coverslips and allowed to adhere. In the inhibitor studies, compounds were added to the media and cells were pre-incubated for 1 h prior to wounding. A single wound was made using a plastic pipette tip through the confluent monolayer and media were changed. For the ezrin studies, a wild-type or T567A VSVG-tagged ezrin construct was microinjected into the nuclei of confluent cells using an Eppendorf system, along with a Cy3-labelled anti-transferrin IgG for the subsequent identification of injected cells. Monolayers were then wounded in such a way that most of the injected cells would remain at the wound edge. Cell migration at the wound edge was recorded overnight at a 5 min lapse interval using a 10× objective, and the images were acquired using Kinetic Imaging (Merseyside, UK) AQM software.

Cell tracking and statistical analysis of migration

Cell trajectories were acquired by manually tracking all the cells over the sequence of time-lapse digital images (Motion Analysis, Kinetic Imaging, Merseyside, UK). The data were used to calculate speed as distance in μm per 5 min and converted to μm per h. Another important aspect of the migration response is the persistence of motility that we measured for each cell as the ratio of the resultant displacement in 16 h over the sum of individual 5 min displacements (Figures 1A and B, and 8). Comparisons between different groups of experiments were made by applying ANOVA to the persistence data. We used ANOVA with a hierarchical and unbalanced model that allows more general testing between treatment groups, and takes into account possible variations between experiments and among different cells in our recordings.

Immunocytochemical staining and confocal microscopy

Immunocytochemical staining was performed as described elsewhere (Kiley and Parker, 1997) except for the following modifications. Cells were permeabilized with 0.2% (v/v) Triton X-100/phosphate-buffered saline (PBS) following fixation in 4% (w/v) paraformaldehyde, with the exception of the slides processed for the GFP–PKCα/VSVG–ezrin association study by FLIM, which were fixed in methanol for 4 min at –20°C, due to the Triton X-100 extractability of some of the ezrin constructs. Cells processed for the determination of ERM C-terminal threonine phosphorylation were first fixed in 10% ice-cold trichloroacetic acid (TCA) as described (Matsui *et al*., 1998). Primary antibodies were diluted 1:200 in PBS containing 1% BSA, except for the fluorophore-conjugated antibodies that were used at 1:20–1:50. The Cy5-labelled anti-rat conjugate was obtained from Jackson ImmunoResearch Laboratories. Confocal images were acquired on a confocal laser scanning microscope (model LSM 510, Carl Zeiss Inc.) equipped with both 40×/1.3Plan-Neofluar and 63×/1.4Plan-Apochromat oil immersion objectives. Each image represents a two-dimensional projection of 2–3 slices in the Z-series, taken across the mid-depth of the cell at 0.2 μm intervals.

FRET determination by FLIM measurements

A detailed description of the FLIM apparatus used for FRET determination in this work can be found elsewhere (Squire and Bastiaens, 1999). The lifetime instrument performs phase- and modulation-based imaging fluorimetry by microscopy. All images were taken using a Zeiss Plan-Apochromat 100×/1.4NA phase 3 oil objective and the homodyne phase-sensitive images recorded at a modulation frequency of 80.224 MHz. The donor (GFP–PKCα) was excited using the 488 nm line of an argon–krypton laser and the resultant fluorescence separated using a combination of dichroic beamsplitter (Q 505 LP; Chroma Technology Corp.) and narrow band emitter filter (BP514/10; Lys and Optik). Acceptor images (Cy3-conjugated IgG or Fabs) were recorded using a 100 W mercury arc lamp (Zeiss Attoarc) as a source of sample illumination combined with a high Q Cy3 filter set (exciter: HQ 535/50, dichroic: Q 565 LP, emitter: HQ 610/75 LP; Chroma Technology Corp.). Global analysis was performed to calculate the precise fraction of donor molecules that have a reduced lifetime due to FRET (i.e. the fraction of GFP–PKCα RD + V3 bound to ezrin) as described (Verveer *et al*., 2000a,b).

Cellular fractionation by sucrose gradient centrifugation

GFP–PKCα-transfected MCF-7 cells were scraped from plates, washed and homogenized using a cell cracker in 0.25 M sucrose, 10 mM HEPES–KOH pH 7.2 containing 1 mM EDTA and 1 mM magnesium acetate. The post-nuclear supernatant was loaded onto a velocity gradient as described (Dittie *et al*., 1997). PKCα and β1 integrin were enriched in VG fractions 2 and 3 (T.Ng and P.J.Parker, unpublished data). EG fractions were subsequently prepared from these VG fractions as described (Dittie *et al*., 1997). Proteins were precipitated from these fractions in 10% TCA overnight, washed with ethanol/acetone (50/50), then denatured in Laemmli's sample buffer, separated on an 8% polyacrylamide gel under reducing conditions and transferred electrophoretically to a polyvinylidene difluoride (PVDF) membrane. Incubation with primary antibodies was performed overnight at 4°C. Detection was with enhanced chemiluminescence (ECL; Amersham) according to recommended procedures.

Immunoprecipitation and western blotting

GFP-tagged or endogenous PKCα was immunoprecipitated from whole-cell lysates (each derived from an 80% confluent cell monolayer in a 15 cm round tissue culture dish, pre-treated with 1 μM PDBu for 20 min) using 10–20 μg of protein G-coupled MC5 as described previously (Kanner *et al*., 1989), except that 1% (w/v) *n*-octyl β-D-glucopyranoside was used instead of NP-40. The samples were separated on large 8% resolving polyacrylamide gels. Blots were then probed with a rabbit IgG that recognizes anti-CPERM (in 0.1% TBS-Tween containing 3% BSA) followed by an anti-rabbit-horseradish peroxidase (HRP) conjugate (Amersham). The same membrane was stripped and reprobed (according to procedures recommended by Amersham) with an affinity-purified rabbit anti-ezrin IgG, then subsequently with an anti-PKCα C-terminal polyclonal serum. Incubation with primary antibodies was performed overnight at 4°C. Detection was with ECL according to recommended procedures.

Immunogold electron microscopy

Cells were scraped carefully and fixed in 4% paraformaldehyde for 1 h, before being processed for routine sectioning on a Leica ultra-cryotome for immunolabelling. Single and double labelling was carried out as described previously (Slot and Geuze, 1985). In the double labelling, the first antibody used was an affinity-purified rabbit polyclonal anti-ezrin IgG (cross-adsorbed against moesin and radixin) recognized by 10 nm PAG; this was followed, after an additional glutaraldehyde fixation step (1% monomeric glutaraldehyde for 5 min to cross-link the primary antibody), by a rabbit anti-GFP antiserum (a kind gift of D.Shima, ICRF) detected with 5 nm PAG. In some studies, the second antibody was omitted to control for cross-reactivity of the 5 nm PAG with the first antibody. After antibody labelling, sections were examined using a Jeol 1010 microscope.

In vitro kinase assays with recombinant or PKCα-co-precipitated endogenous ezrin

The potential phosphorylation of GST-tagged full-length ezrin by PKCα was examined in an *in vitro* ^{32}P incorporation assay where 5 μl (0.27 μg) of human recombinant PKCα (PanVera Corporation) were put in a 35 μl reaction buffer containing 5 μl (1.7 μg) of GST–ezrin, 5 μl (0.8 mM) of ATP containing 1 μCi of [^{32}P]ATP (255 c.p.m./pmol), 5 μl each of $MgCl_2$ (0.1 M) and $CaCl_2$ (6 mM), 10 μl of a pure lipid sonicated suspension of 50 μg of phosphatidylserine, 5 μg of phosphatidylinositol 4,5-bis-

phosphate and 0.05 μg of TPA in 0.2 M HEPES pH 7.5/2 mM EGTA. The control reaction was carried out in the absence of lipids/TPA. The *in vitro* phosphorylation reactions were incubated at 30°C and stopped after various time points by adding 40 μl of modified Laemmli's sample buffer (containing final concentrations of 2% SDS, 4 M urea and 10 mM EDTA). The samples were then separated on an 8% polyacrylamide gel and the phosphorylated proteins were detected by autoradiography. The *in vitro* phosphorylation assay was also performed with protein G–agarose bead-bound, PKCα-co-precipitated endogenous ERM (see the legend of Figure 7B for experimental details).

Acknowledgements

We wish to thank Dr Gipi Schiavo and Professor Ian Hart (ICRF) for their valuable comments. 2C4 fibrosarcoma cells stably expressing GFP–PKCα (GFP–PKCα-2C4) or GFP control vector were kindly provided by B.Lillemeier. We also thank Professor Clare Isacke (Imperial College, London) and Professor Paul Mangeat (Universite Montpellier II, Montpellier) for kindly providing the GST-tagged ezrin plasmid and crude sera against radixin and moesin, respectively. We thank Christine T.Quang for many helpful discussions. This study was supported by the Imperial Cancer Research Fund (UK) and the UK Medical Research Council (in the form of a Clinician Scientist Grant awarded to T.N.).

References

Algrain,M., Turunen,O., Vaheri,A., Louvard,D. and Arpin,M. (1993) Ezrin contains cytoskeleton and membrane binding domains accounting for its proposed role as a membrane–cytoskeletal linker. *J. Cell Biol.*, **120**, 129–139.

Arber,S., Barbayannis,F.A., Hanser,H., Schneider,C., Stanyon,C.A., Bernard,O. and Caroni,P. (1998) Regulation of actin dynamics through phosphorylation of cofilin by LIM-kinase. *Nature*, **393**, 805–809.

Bae,Y.S., Cantley,L.G., Chen,C.S., Kim,S.R., Kwon,K.S. and Rhee,S.G. (1998) Activation of phospholipase C-γ by phosphatidylinositol 3,4,5-trisphosphate. *J. Biol. Chem.*, **273**, 4465–4469.

Bastiaens,P.I.H. and Jovin,T.M. (1998) Fluorescence resonance energy transfer microscopy. In Celis,J. (ed.), *Cell Biology: A Laboratory Handbook*. Academic Press, New York, NY, pp. 136–146.

Berrier,A.L., Mastrangelo,A.M., Downward,J., Ginsberg,M. and LaFlamme,S.E. (2000) Activated R-Ras, Rac1, PI 3-kinase and PKCε can each restore cell spreading inhibited by isolated integrin β1 cytoplasmic domains. *J. Cell Biol.*, **151**, 1549–1560.

Bretscher,A., Chambers,D., Nguyen,R. and Reczek,D. (2000) ERM-Merlin and EBP50 protein families in plasma membrane organization and function. *Annu. Rev. Cell Dev. Biol.*, **16**, 113–143.

Bruns,R.F., Miller,F.D., Merriman,R.L., Howbert,J.J., Heath,W.F., Kobayashi,E., Takahashi,I., Tamaoki,T. and Nakano,H. (1991) Inhibition of protein kinase C by calphostin C is light-dependent. *Biochem. Biophys. Res. Commun.*, **176**, 288–293.

Buchanan,F.G., Elliot,C.M., Gibbs,M. and Exton,J.H. (2000) Translocation of the Rac1 guanine nucleotide exchange factor Tiam1 induced by platelet-derived growth factor and lysophosphatidic acid. *J. Biol. Chem.*, **275**, 9742–9748.

Cazaubon,S., Bornancin,F. and Parker,P.J. (1994) Threonine-497 is a critical site for permissive activation of protein kinase Cα. *Biochem. J.*, **301**, 443–448.

Crepaldi,T., Gautreau,A., Comoglio,P.M., Louvard,D. and Arpin,M. (1997) Ezrin is an effector of hepatocyte growth factor-mediated migration and morphogenesis in epithelial cells. *J. Cell Biol.*, **138**, 423–434.

Derman,M.P., Toker,A., Hartwig,J.H., Spokes,K., Falck,J.R., Chen,C.S., Cantley,L.C. and Cantley,L.G. (1997) The lipid products of phosphoinositide 3-kinase increase cell motility through protein kinase C. *J. Biol. Chem.*, **272**, 6465–6470.

Dittie,A.S., Thomas,L., Thomas,G. and Tooze,S.A. (1997) Interaction of furin in immature secretory granules from neuroendocrine cells with the AP-1 adaptor complex is modulated by casein kinase II phosphorylation. *EMBO J.*, **16**, 4859–4870.

Gautreau,A., Poullet,P., Louvard,D. and Arpin,M. (1999) Ezrin, a plasma membrane–microfilament linker, signals cell survival through the phosphatdiylinositol 3-kinase/Akt pathway. *Proc. Natl Acad. Sci. USA*, **96**, 7300–7305.

Gautreau,A., Louvard,D. and Arpin,M. (2000) Morphogenic effects of ezrin require a phosphorylation-induced transition from oligomers to monomers at the plasma membrane. *J. Cell Biol.*, **150**, 193–203.

Imamura,H., Takaishi,K., Nakano,K., Kodama,A., Oishi,H., Shiozaki,H., Monden,M., Sasaki,T. and Takai,Y. (1998) Rho and Rab small G proteins coordinately reorganize stress fibers and focal adhesions in MDCK cells. *Mol. Biol. Cell*, **9**, 2561–2575.

Ishizaki,T., Uehata,M., Tamechika,I., Keel,J., Nonomura,K., Maekawa,M. and Narumiya,S. (2000) Pharmacological properties of Y-27632, a specific inhibitor of rho-associated kinases. *Mol. Pharmacol.*, **57**, 976–983.

Kanner,S.B., Reynolds,A.B. and Parsons,J.T. (1989) Immunoaffinity purification of tyrosine-phosphorylated cellular proteins. *J. Immunol. Methods*, **120**, 115–124.

Kiley,S.C. and Parker,P.J. (1997) Defective microtubule reorganization in phorbol ester-resistant U937 variants: reconstitution of the normal cell phenotype with nocodazole treatment. *Cell Growth Differ.*, **8**, 231–242.

Kiley,S.C., Clark,K.J., Goodnough,M., Welch,D.R. and Jaken,S. (1999) Protein kinase Cδ involvement in mammary tumor cell metastasis. *Cancer Res.*, **59**, 3230–3238.

Lamb,R.F., Ozanne,B.W., Roy,C., McGarry,L., Stipp,C., Mangeat,P. and Jay,D.G. (1997) Essential functions of ezrin in maintenance of cell shape lamellipodial extension in normal and transformed fibroblasts. *Curr. Biol.*, **7**, 682–688.

Mangeat,P., Roy,C. and Martin,M. (1999) ERM proteins in cell adhesion and membrane dynamics. *Trends Cell Biol.*, **9**, 187–192.

Matsui,T., Maeda,M., Doi,Y., Yonemura,S., Amano,M., Kaibuchi,K. and Tsukita,S. (1998) Rho-kinase phosphorylates COOH-terminal threonines of ezrin/radixin/moesin (ERM) proteins and regulates their head-to-tail association. *J. Cell Biol.*, **140**, 647–657.

Matsui,T., Yonemura,S. and Tsukita,S. (1999) Activation of ERM proteins *in vivo* by Rho involves phosphatidylinositol 4-phosphate 5-kinase and not ROCK kinases. *Curr. Biol.*, **9**, 1259–1262.

Meng,F. and Lowell,C.A. (1998) A β1 integrin signaling pathway involving Src-family kinases, Cbl and PI-3 kinase is required for macrophage spreading and migration. *EMBO J.*, **17**, 4391–4403.

Nakamura,F., Huang,L., Pestonjamasp,K., Luna,E.J. and Furthmayr,H. (1999) Regulation of F-actin binding to platelet moesin *in vitro* by both phosphorylation of threonine 558 and polyphosphatidylinositides. *Mol. Biol. Cell*, **10**, 2669–2685.

Ng,T., Shima,D., Squire,A., Bastiaens,P.I.H., Gschmeissner,S., Humphries, M.J. and Parker,P.J. (1999a) PKCα regulates β1 integrin-dependent motility, through association and control of integrin traffic. *EMBO J.*, **18**, 3909–3923.

Ng,T. *et al*. (1999b) Imaging PKCα activation in cells. *Science*, **283**, 2085–2089.

Pearson,M.A., Reczek,D., Bretscher,A. and Karplus,P.A. (2000) Structure of the ERM protein moesin reveals the FERM domain fold masked by an extended actin binding tail domain. *Cell*, **101**, 259–270.

Pietromonaco,S.F., Simons,P.C., Altman,A. and Elias,L. (1998) Protein kinase C-θ phosphorylation of moesin in the actin-binding sequence. *J. Biol. Chem.*, **273**, 7594–7603.

Platet,N., Prevostel,C., Derocq,D., Joubert,D., Rochefort,H. and Garcia,M. (1998) Breast cancer cell invasiveness: correlation with protein kinase C activity and differential regulation by phorbol ester in estrogen receptor-positive and -negative cells. *Int. J. Cancer*, **75**, 750–756.

Shaw,L.M., Rabinovitz,I., Wang,H.H.F., Toker,A. and Mercurio,A.M. (1997) Activation of phosphoinositide 3-OH kinase by the α6β4 integrin promotes carcinoma invasion. *Cell*, **91**, 949–960.

Slot,J.W. and Geuze,H.J. (1985) A new method of preparing gold probes for multiple-labeling cytochemistry. *Eur. J. Cell Biol.*, **38**, 87–93.

Squire,A. and Bastiaens,P.I. (1999) Three dimensional image restoration in fluorescence lifetime imaging microscopy. *J. Microsc.*, **193**, 36–49.

Steiner,B. *et al*. (1990) Phosphorylation of microtubule-associated protein tau: identification of the site for Ca^{2+}-calmodulin dependent kinase and relationship with tau phosphorylation in Alzheimer tangles. *EMBO J.*, **9**, 3539–3544.

Sun,X.G. and Rotenberg,S.A. (1999) Overexpression of protein kinase C α in MCF-10A human breast cells engenders dramatic alterations in morphology, proliferation and motility. *Cell Growth Differ.*, **10**, 342–352.

Surtees,G. (1964) Laboratory studies on dispersion behaviour of adult beetles in grain. VIII Spontaneous activity in three species and a new approach to analysis of kinetic mechanism. *Anim. Behav.*, **12**, 374.

Tang,S., Morgan,K.G., Parker,C. and Ware,J.A. (1997) Requirement for

protein kinase C θ for cell cycle progression and formation of actin stress fibers and filopodia in vascular endothelial cells. *J. Biol. Chem.*, **272**, 28704–28711.

Tran Quang,C., Gautreau,A., Arpin,M. and Treisman,R. (2000) Ezrin function is required for ROCK-mediated fibroblast transformation by the Net and Dbl oncogenes. *EMBO J.*, **19**, 4565–4576.

Tsukita,S. and Yonemura,S. (1999) Cortical actin organization: lessons from ERM (ezrin/radixin/moesin) proteins. *J. Biol. Chem.*, **274**, 34507–34510.

Vanhaesebroeck,B., Jones,G.E., Allen,W.E., Zicha,D., Hooshmand-Rad,R., Sawyer,C., Wells,C., Waterfield,M.D. and Ridley,A.J. (1999) Distinct PI(3)Ks mediate mitogenic signalling and cell migration in macrophages. *Nature Cell Biol.*, **1**, 69–71.

Verveer,P.J., Squire,A. and Bastiaens,P.I. (2000a) Global analysis of fluorescence lifetime imaging microscopy data. *Biophys. J.*, **78**, 2127–2137.

Verveer,P.J., Wouters,F.S., Reynolds,A.R. and Bastiaens,P.I. (2000b) Quantitative imaging of lateral ErbB1 receptor signal propagation in the plasma membrane. *Science*, **290**, 1567–1570.

Vicente-Manzanares,M. *et al*. (1999) Involvement of phosphatidyl-inositol 3-kinase in stromal cell-derived factor-1-α-induced lymphocyte polarization and chemotaxis. *J. Immunol.*, **163**, 4001–4012.

Wallis,S., Lloyd,S., Wise,I., Ireland,G., Fleming,T.P. and Garrod,D. (2000) The α isoform of protein kinase C is involved in signaling the response of desmosomes to wounding in cultured epithelial cells. *Mol. Biol. Cell*, **11**, 1077–1092.

Wang,M.H., Montero-Julian,F.A., Dauny,I. and Leonard,E.J. (1996) Requirement of phosphatidylinositol-3 kinase for epithelial cell migration activated by human macrophage stimulating protein. *Oncogene*, **13**, 2167–2175.

Young,S., Rothbard,J. and Parker,P.J. (1988) A monoclonal antibody recognising the site of limited proteolysis of protein kinase C. Inhibition of down-regulation *in vivo*. *Eur. J. Biochem.*, **173**, 247–252.

Zigmond,S.H. (1996) Signal transduction and actin filament organization. *Curr. Opin. Cell Biol.*, **8**, 66–73.

Received November 30, 2000; revised and accepted April 5, 2001